UC-413

LBL-27831

Lawrence Berkeley Laboratory

UNIVERSITY OF CALIFORNIA

Presented at the American Physical Society Symposium on Exotic Nuclear Spectroscopy, Miami Beach, FL, September 10–15, 1989, and to be published in the *ACS Symposium Series*

Delayed Fission of Light Americium Isotopes

H.L. Hall and D.C. Hoffman

October 1989

NUCLEAR SCIENCE DIVISION

For Reference

Not to be taken from this room

LBL-27831 Copy 1 Bldg. 50 Library.

Prepared for the U.S. Department of Energy under Contract Number DE-AC03-76SF00098.

DISCLAIMER

This document was prepared as an account of work sponsored by the United States Government. While this document is believed to contain correct information, neither the United States Government nor any agency thereof, nor the Regents of the University of California, nor any of their employees, makes any warranty, express or implied, or assumes any legal responsibility for the accuracy, completeness, or usefulness of any information, apparatus, product, or process disclosed, or represents that its use would not infringe privately owned rights. Reference herein to any specific commercial product, process, or service by its trade name, trademark, manufacturer, or otherwise, does not necessarily constitute or imply its endorsement, recommendation, or favoring by the United States Government or any agency thereof, or the Regents of the University of California. The views and opinions of authors expressed herein do not necessarily state or reflect those of the United States Government or any agency thereof or the Regents of the University of California.

LBL-27831

Delayed Fission of Light Americium Isotopes

H. L. Hall† and D. C. Hoffman

Department of Chemistry
University of California
Berkeley, CA 94720

and

Nuclear Science Division
Lawrence Berkeley Laboratory
1 Cyclotron Road
Berkeley, CA 94720

October 2, 1989

This work was supported in part by the Director, Office of Energy Research, Division of Nuclear Physics of the Office of High Energy and Nuclear Physics of the U.S. Department of Energy under Contract DE-AC03-76SF00098.

†Bitnet: **HLHall@LBL.gov**

Abstract

Fission characteristics of the delayed-fission decay mode in light americium nuclei have been investigated. Total kinetic energy and mass-yield distributions were measured for ^{232}Am and for ^{234}Am, and delayed-fission probabilities of 6.9×10^{-4} and 6.6×10^{-5}, respectively, were determined. The total kinetic energy and the asymmetric mass-yield distributions are typical of fission of mid-range actinides. No discernible influence of the anomalous triple-peaked mass division characteristic of the thorium-radium region was detected. Measurements of the time correlation between the electron-capture x-rays and the subsequent fission confirm that the observed fissions arise from the electron-capture delayed-fission mechanism.

1 Introduction

Delayed fission (DF) is a nuclear decay process in which a decaying nucleus populates excited states in its daughter nucleus, which then fission. These states can be above the fission barrier(s) of the daughter (yielding prompt fission), within the second well of the potential energy surface (a fission shape isomer), or within the first well of the potential energy surface (an electromagnetic isomer). This is illustrated schematically in Figure 1. This decay mode is believed to influence the production yields of heavy elements in multiple neutron capture processes [1, 2, 3, 4, 5] followed by β decay, such as in the astrophysical r-process and in thermonuclear weapons tests. Delayed-fission processes may also provide a sensitive probe of fission barriers in the heavy element region [6].

The probability of this decay mode, P_{DF}, can be expressed in terms of experimentally measurable quantities as

$$P_{DF} = \frac{N_{if}}{N_i} \tag{1}$$

where N_i is the number of the type of decays of interest (*e.g.*, β^- or EC) and N_{if} is the number of those decays leading to delayed fission. P_{DF} can be derived from statistical considerations as

$$P_{DF} = \frac{\int_0^{Q_i} W_i(Q_i - E)\frac{\Gamma_f}{\Gamma_f+\Gamma_\gamma}(E)dE}{\int_0^{Q_i} W_i(Q_i - E)dE}, \tag{2}$$

where $W_i(E)$ is the transition probability function for the decay of interest, $\frac{\Gamma_f}{\Gamma_f+\Gamma_\gamma}(E)$ is the ratio of the fission width of excited levels within the daughter nucleus to the total depopulation width of these states, E is the excitation energy of the daughter nucleus, and Q_i is the Q-value for the decay mode of interest. It is assumed that no decay channels are open to the excited states other than fission and γ decay, so that $(\Gamma_\gamma + \Gamma_f)$ is the total decay width of the excited states.

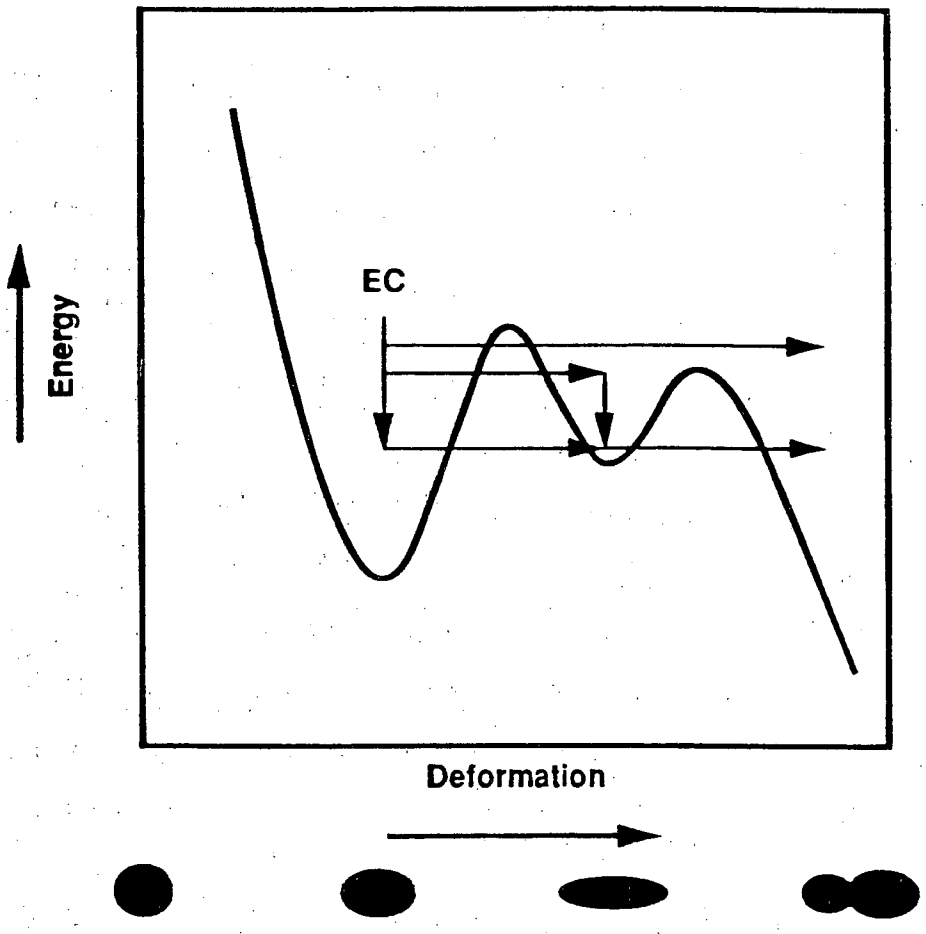

Figure 1: Schematic illustration of the delayed-fission process.

P_{DF} is strongly dependent on the energy available for the decay and the structure of the fission barrier, primarily due to the fission-width term, $\frac{\Gamma_f}{\Gamma_f+\Gamma_\gamma}(E)$. The γ-decay term, Γ_γ, can be estimated from semi-empirical relationships [7] to be

$$\Gamma_\gamma = \frac{C_\gamma \Theta^4 e^{(E/\Theta)}}{2\pi\rho}, \tag{3}$$

where ρ is the nuclear level density, C_γ is a constant, and Θ is the nuclear temperature. The fission width, Γ_f, derived from the penetrability of the fission barrier with several simplifying assumptions [8], is qualitatively described by

$$\Gamma_f = \frac{R_B}{2\pi\rho}(1 + e^{\frac{2\pi(B_f - E)}{h\omega_f}})^{-1} \tag{4}$$

where R_B is the penetrability of the outer fission barrier from the lowest-lying state in the second well, ρ is the level density in the inner well, B_f is the height of the inner fission barrier, and $h\omega_f$ is the energy associated with the inner barrier curvature.

As a result, Γ_f is expected to be exponentially dependent on the difference between the fission barrier and the Q-value (which enters as the upper limit of the integrals in Equation (2)). Hence, for the study of EC-delayed fission in the actinide region, it is necessary to choose nuclei for which Q_ε is comparable to the fission barrier (about 4-6 MeV). This requires study of nuclei far from the valley of β-stability, which introduces a number of experimental difficulties in the production and characterization of these nuclei.

It should be noted that the above equations neglect the contribution of discrete nuclear structure in the daughter nucleus to the delayed-fission probability. The simplifications discussed above and in more detail in Ref. [8] are based on the assumption that decay to the daughter nucleus proceeds to sufficiently energetic states that the system can be treated statistically. However, the low-lying structure [9] of the daughter can either promote or hinder the delayed-fission mechanism. For example, β-delayed fission in ^{256m}Es has been observed [10] to proceed from a single level at 1425 keV in the daughter

^{256}Fm. One would not normally expect fission from a level so close to the daughter's ground state, but γ decay from this level was heavily hindered (level half-life ~70 ns) so that fission was able to compete successfully with γ decay. As a result, the P_{DF} for ^{256m}Es was observed to be 2×10^{-5}. On the other hand, a nucleus with a high Q_ε might be expected to have a large P_{DF}, but if electron capture to the ground state is super-allowed ($\Delta I^{\Delta\pi} = 0^{\mathrm{No}}$) essentially no high-lying states might be populated. Recent theoretical models [5, 9] incorporate structural information in the β-strength function (a term in $W_i(E)$).

2 History

Anomalous fission activities were first observed [11, 12] in the light americium and neptunium regions as early as 1966. In 1969, Berlovich and Novikov [13] noted that this region met the conditions required for delayed fission, although the observed fissions were not specifically attributed [14] to delayed-fission processes until 1972. A 55 second fission activity, attributed to εDF in ^{232}Am, was reported by Habs *et al.* [15] in 1978, and the P_{DF} for this isotope was reported to be on the order of one percent. An εDF branch has been tentatively assigned [16] to ^{242}Es, again with a P_{DF} on the order of one percent. Recently, εDF has been reported [17] outside the actinide elements, in the region of ^{180}Hg.

Most studies to date have reported only half-life and fission cross-section (σ_f) data measured without any separation of the delayed-fissile species from other reaction products. The electron-capture cross section (σ_ε), when reported, has generally been extracted from theoretical calculations or systematics, not measured experimentally. Gangrskiĭ *et al.* [7] report delayed-fission probabilities for several transcurium nuclei using the measured α decay of the EC daughter to estimate σ_ε, by assuming the observed fission activity does

arise from the same parent. All reports of εDF are summarized in Table 1.

β-delayed fission (βDF) has been postulated to play a role in multiple neutron-capture processes. Burbidge, Burbidge, Fowler and Hoyle [1] proposed βDF as a route for depleting the yield of heavy elements produced in supernovae. βDF is one possible explanation of why superheavy elements are not found in nature [2, 3]. βDF had once been predicted to significantly influence heavy-element yields in thermonuclear weapons tests [2, 3]; however, analyses of experimental data [20, 21] show that the predicted delayed-fission effects are seriously overestimated.

The first report of an observed fission activity attributed to β-delayed fission appeared in 1978 when ^{236}Pa and ^{238}Pa were reported by Gangrskiĭ *et al.* [22] to exhibit βDF with probabilities of about 10^{-10} and $10^{-6.2}$, respectively. Gangrskiĭ *et al.* performed no chemical separation of the two protactinium isotopes produced in irradiations of uranium foils. Subsequently, Baas-May *et al.* [23] studied ^{238}Pa using automated chemical separation procedures and observed no βDF from this isotope. They set an upper limit on the delayed-fission probability for ^{238}Pa of $P_{DF} \leq 2.6 \times 10^{-8}$. This failure to confirm βDF in ^{238}Pa cast considerable doubt on the earlier report [22] of a βDF branch in ^{236}Pa, since both ^{236}Pa and ^{238}Pa were measured in a similar fashion. ^{256m}Es is the most recently identified [10] β-delayed fissile species, and is also the first case in which the fissioning isomeric level in the daughter nucleus has been assigned. A summary of experimental reports of βDF is presented in Table 2.

3 Selection of the Am Region

The neutron-deficient americium region was selected for the present study for several reasons. First, there are already two isotopes in this region with reported delayed-fission branches (See Table 1), ^{232}Am and ^{234}Am. The

Table 1: Summary of reported observations of EC-delayed fission (does not include measurements presented in this work).

Nuclide[a]	$t_{1/2}$[b]	P_{DF}[c]	Reference
^{250}Md	52 sec.	2×10^{-4}	Gangrskiĭ 1980 [7]
^{248}Es	28 min.	3×10^{-7}	Gangrskiĭ 1980 [7]
^{246}Es	8 min.	3×10^{-5}	Gangrskiĭ 1980 [7]
^{244}Es	37 sec.	10^{-4}	Gangrskiĭ 1980 [7]
^{242}Es?	5 - 25 sec.	$(1.4 \pm 0.8) \times 10^{-2}$	Hingmann 1985 [16]
^{240}Bk	4 min.	10^{-5}	Gangrskiĭ 1980 [7]
^{234}Am	2.6 ± 0.2 min.	NR[d,e]	Skobelev 1972 [14]
^{234}Am	2.6 ± 0.2 min.	NR	Somerville 1977 [18]
^{232}Am	1.4 ± 0.25 min.	NR[e]	Skobelev 1972 [14]
^{232}Am	0.92 ± 0.12 min.	$1.3^{+4}_{-0.8} \times 10^{-2}$	Habs 1978 [15]
^{228}Np	60 ± 5 sec.	NR	Skobelev 1972 [14]
^{180}Tl?	$0.70^{+0.12}_{-0.09}$ sec.	$\approx 10^{-6}$	Lazarev 1987 [17]

[a]The parent nuclide undergoing EC decay to excited states in the daughter which then fission is given.
[b]Half-life is given as reported, or converted to a common unit when multiple references exist.
[c]Errors limits are given if reported.
[d]Not reported.
[e]Kuznetsov [19] subsequently used the reported fission cross sections and calculated P_{DF} for ^{232,234}Am using an evaporation code to estimate the EC cross section. The values obtained were 6.96×10^{-2} and 6.95×10^{-5}, respectively.

Table 2: Summary of reported observations of β-delayed fission.

Nuclide[a]	$t_{1/2}$[b]	P_{DF}	Reference
^{256m}Es	7.6 hour	2×10^{-5}	Hall 1989 [10]
^{238}Pa[c]	2.3 min.	6×10^{-7}	Gangrskiĭ 1978 [22]
^{238}Pa[d]	2.3 min.	$\approx 10^{-8}$	Gangrskiĭ 1978 [22]
^{238}Pa[c]	2.3 min.	$\leq 2.6 \times 10^{-8}$	Baas-May 1985 [23]
^{236}Pa[e]	9.1 min.	$\approx 10^{-9}$	Gangrskiĭ 1978 [22]
^{236}Pa[f]	9.1 min.	3×10^{-10}	Gangrskiĭ 1978 [22]

[a]The parent nuclide undergoing β decay to excited states in the daughter which then fission is given.
[b]Half-life is given as reported, or converted to a common unit when multiple references exist.
[c]Produced via ^{238}U(14.7-MeV n,p).
[d]Produced via ^{238}U(8–20-MeV n,p).
[e]Produced via ^{238}U(27-MeV γ,np).
[f]Produced via ^{238}U(18-MeV d,α).

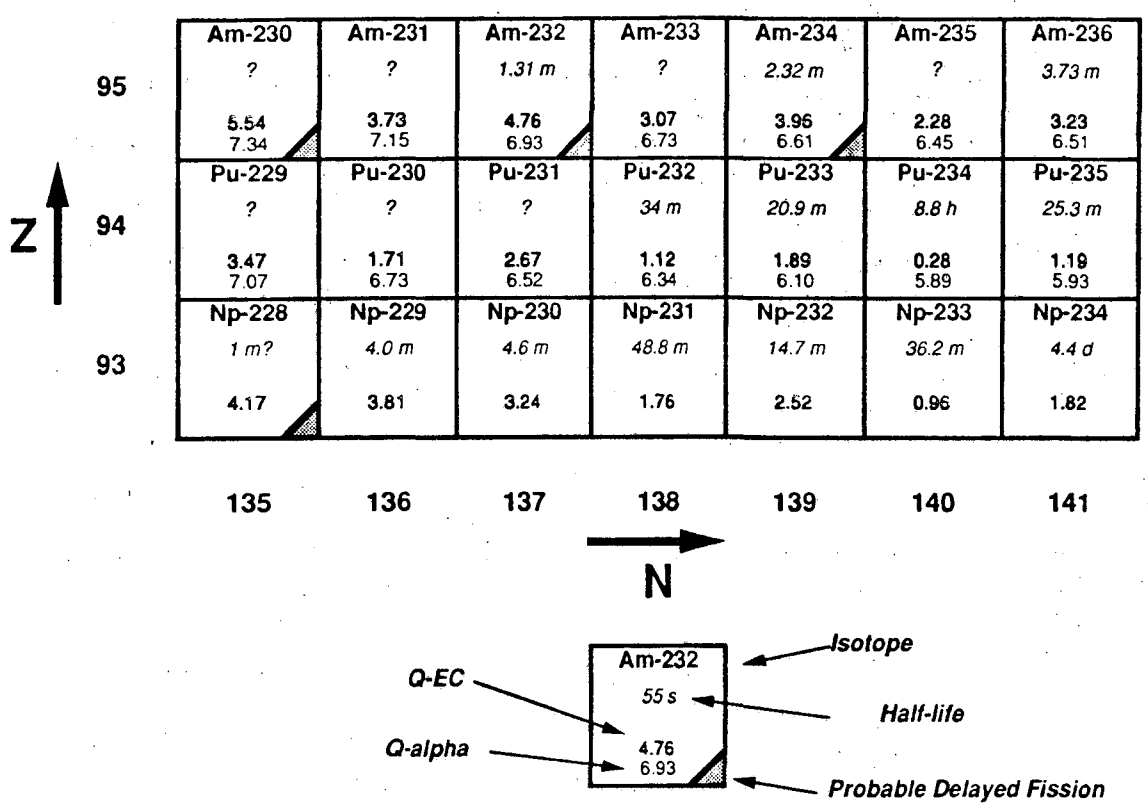

Figure 2: The neutron-deficient americium region of the chart of the nuclides.

εDF branch in ^{232}Am was reported [15] to be approximately 1%, while no measurement of P_{DF} was reported [14] for ^{234}Am although Kuznetsov [19] had estimated it to be 7×10^{-5} from the data in Reference [14]. Also, using the systematic approach of Habs *et al.* [15] and a Q_ε of 3.96 MeV for ^{234}Am (calculated using the masses of Möller, Myers, Świątecki, and Treiner [24]), P_{DF} for ^{234}Am was estimated [8] to be on the order of 10^{-4} to 10^{-5}.

Secondly, these two isotopes are reported to have half-lives long enough (reported as 55 sec [15] and 2.6 min [14], respectively) that rapid radiochemical separations can be performed on them. With rapid radiochemical separations, an americium fraction can be purified sufficiently to allow observation of the K-capture x-rays from the decay of americium to plutonium without excessive γ interference. This would allow determination of the EC cross-section experimentally, yielding half of the data required to determine P_{DF} by Equation (1).

Third, the recent development [25] of the Light Ion Multiple Target System (**LIM** Target System) allows the use of multiple targets with high yield of the reaction products, so up to twelve ^{237}Np targets can be irradiated at a time. This target system is illustrated in Figure 3. Since the fission production rate increases linearly with the number of targets irradiated, this would allow detection of a sufficient number of fissions to measure both the total kinetic energy (TKE) and mass-yield distributions of the εDF mode.

Measurement of the TKE and mass-yield distributions is important because εDF has the potential to vastly expand the number of nuclei in which low-energy fission [26, 27, 28, 29] can be studied. This very low excitation-energy fission mode is essentially inaccessible for neutron-deficient species this far from stability with common techniques such as (n,f) and charged-particle reactions unless the nuclei in question spontaneously fission. This is not the case for the light actinides. Low excitation energy fission data may assist in understanding the dynamics of the fission process as the excitation

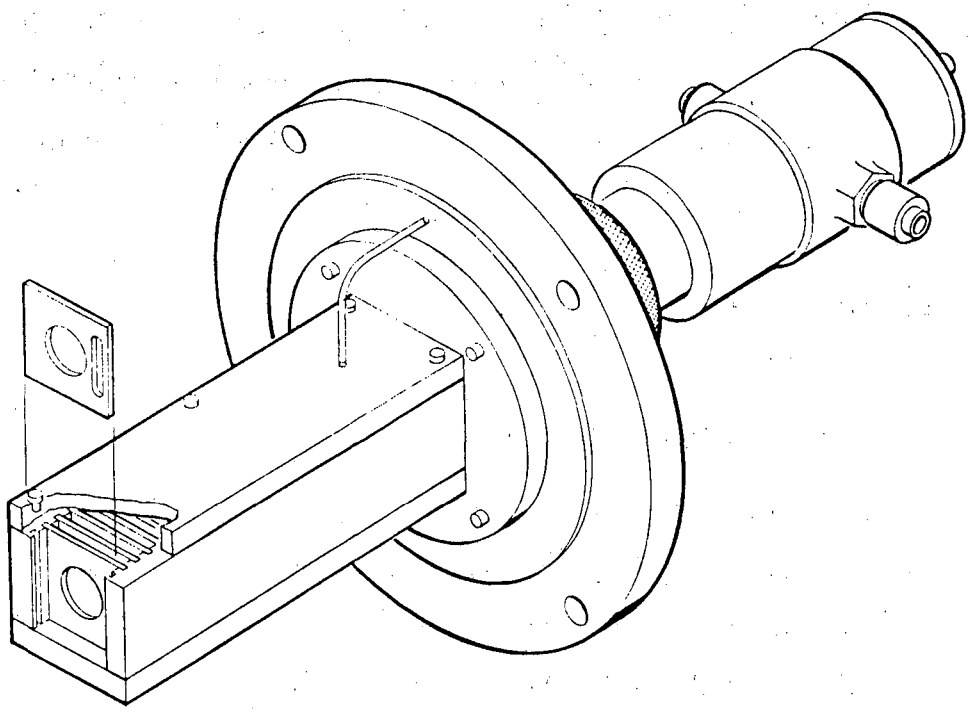

Figure 3: Illustration of the multiple target system developed [25] for these studies.

energy of the fissioning nucleus goes to zero, leading to ground-state fission.

Finally, the light americium region is nearly isotonic with nuclei displaying the "thorium anomaly," *i.e.*, triple-humped mass-yield distributions [30-33] from neutron-induced fission. Since εDF in the light americium region may be in the transition region between the Th-anomaly and the "normal" double-humped mass-yield distributions of the mid-range actinides, its fission properties may provide clues to understanding the Th-anomaly. Since εDF cannot bring more excitation energy into the nucleus than the Q_ε-value, the influences of excitation energy on the fission properties are minimized.

4 Experimental

4.1 Targets and Irradiations

^{237}Np targets ranging in thicknesses from 125 μg/cm^2 to 200 μg/cm^2 were mounted in the **LIM** [25] Target System, with a spacing of approximately one centimeter between the targets. A 25-μm beryllium foil served as the volume limiting foil, and another 25-μm beryllium foil served as the vacuum window for the system. For the initial studies of the fission properties of ^{232}Am the target backings were 2.5-μm molybdenum. However, because of the highly $\beta\gamma$-active byproducts from the reactions of the beam with the molybdenum target backings, a set of targets on 25-μm beryllium foil was used for all subsequent measurements.

The α-particle beams used for this work were provided by the Lawrence Berkeley Laboratory 88-Inch Cyclotron. For the production of ^{232}Am by the ^{237}Np$(\alpha, 9n)$ reaction, the α-particle energy was 99 ± 1.5 MeV on target (all energies are given in the laboratory frame of reference). ^{234}Am was produced via the ^{237}Np$(\alpha, 7n)$ reaction, and the α-particle energy was 72 ± 2 MeV on target. The beam intensity was 2-7 pμA for all irradiations. The recoiling

reaction products were collected on KCl aerosols in helium, which swept out the volume behind each target continuously. The activity-laden aerosols were transported via a polyvinyl chloride capillary tube to either the rotating-wheel system (see **4.2** below) or to a collection site in a chemistry laboratory (see **4.3** below).

4.2 On-line Measurements

For on-line measurements of the fission properties of ^{234}Am, the KCl aerosols were transported about five meters via a capillary tube and collected on a thin ($\sim 40 \pm 15 \mu g/cm^2$) polypropylene foil placed on the periphery of a wheel. At preset intervals the wheel rotated 4.5°, passing the polypropylene foil through a series of six detector stations (each consisting of a pair of ion-implanted passivated silicon detectors on either side of the wheel). This arrangement allowed detection of coincident fission fragments with an efficiency of approximately 60%. Each detector station could also detect α particles, again with a total efficiency of about 60%. Under the conditions of these experiments, the α-particle energy resolution was about 40 keV. The detectors were calibrated for the fission measurements with a ^{252}Cf source on a thin polypropylene foil.

As the data were digitized, each event was tagged with a time and a detector marker, and then written to magnetic tape in list (event-by-event) mode. Subsequent sorting and histogramming were performed on the data to extract α spectra, fission-fragment spectra, coincidence data, and decay information. The rotating wheel is known as the "Merry Go-around" (**MG**), and the controlling computer system and its affiliated electronics are known as the Realtime Acquisition Graphics System (**RAGS**), hence the acronym **MG-RAGS**.

4.3 Chemical Procedures

Two different chemical separations were performed on the reaction products of these irradiations. One separation was designed to assign the Z of the fissioning species to americium (or fission of plutonium following electron capture in americium), and the other was used to produce an americium sample suitable for measurement of the plutonium K x-rays from the EC decay of the americium parent. Measurement of the EC decay in conjunction with the εDF branch would allow determination of P_{DF} experimentally.

4.3.1 Chemical Procedure for Elemental Assignment

In the separation designed to assign the Z of the fissioning activity produced by these reactions, the activity-laden aerosols were transported about five meters via a capillary tube and collected on a tantalum foil. The activity and KCl were then dissolved in 20 μL of 8 **M** HNO_3. The resulting solution was passed through a 1-mm $\times$ 10-mm anion-exchange column (Bio-Rad AG 1-X8, 200-400 mesh). Under these conditions all trivalent actinides will pass through the column, while the higher valence actinides are adsorbed by the resin. The column was washed with $\sim$ 100 μL of 8 **M** HNO_3, and the eluant was collected on a tantalum foil, dried, flamed, and counted with a silicon surface barrier (SSB) detector for α particles and fissions. The column was then washed with $\sim$ 100 μL of 3 **M** HCl – 0.1 **M** HF to elute neptunium and plutonium. This eluant was also collected on a tantalum foil, dried, flamed, and counted. A flow chart of this separation procedure is given in Figure 4. Data from the SSB detectors were stored using **RAGS**. The total time required for this separation was about 90 seconds.

The first fraction contains only the trivalent actinides produced in this reaction, while the second contains any neptunium, plutonium, uranium, protactinium, or thorium produced. Francium, radium, and actinium would follow the americium in this procedure, as would the lanthanides. However,

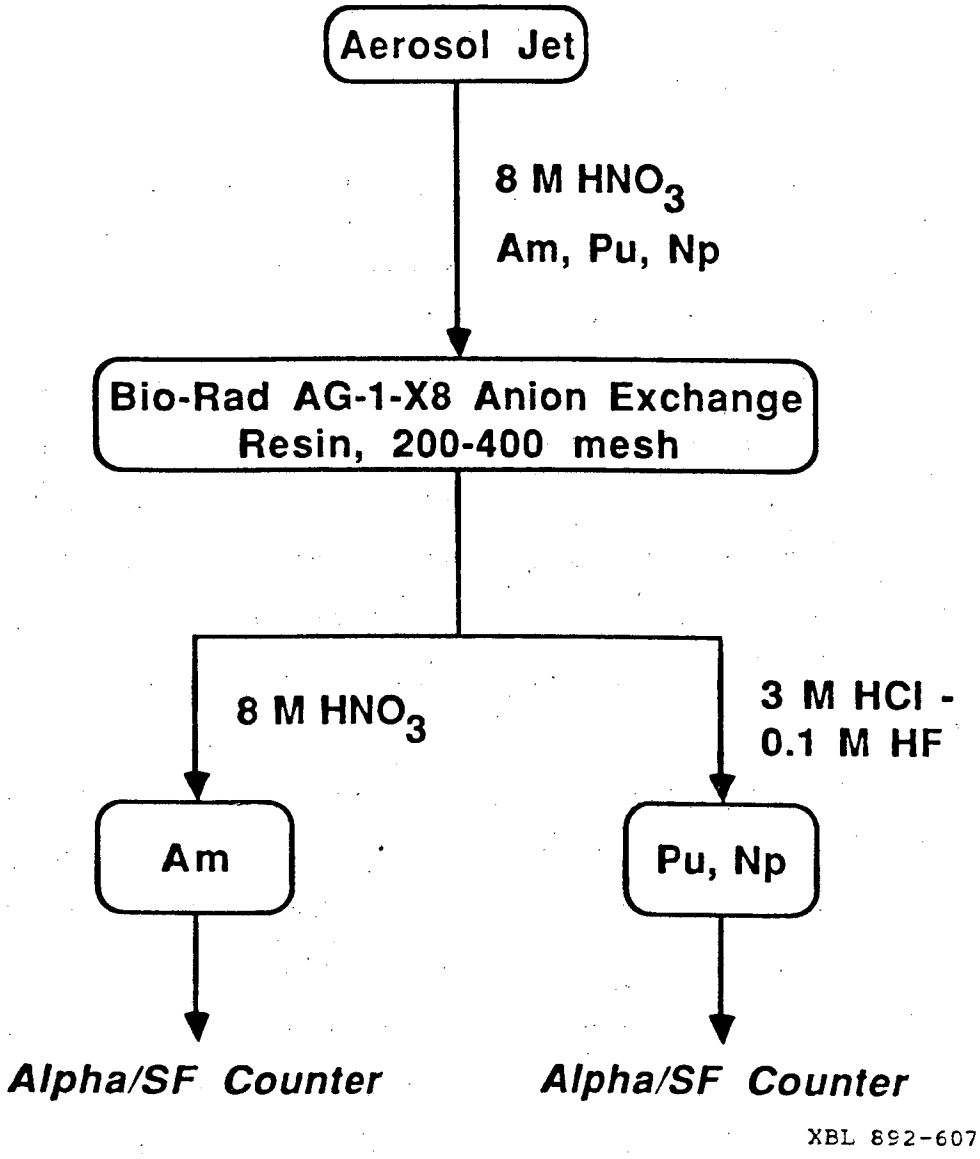

Figure 4: Flow chart of the chemical separation used to confirm the assignment of the fission activity produced in these reactions to americium.

the amount of Fr, Ra, and Ac produced in this reaction was observed (from the on-line α spectra) to be very small, and the lanthanides are unlikely to fission. Hence, americium is the only reasonable elemental assignment for any fission activity observed in the first fraction.

4.3.2 Chemical Procedure for P_{DF} and σ_ε Measurement

This separation procedure had to be more specific for americium since it was necessary to separate americium from highly γ-active fission products formed with production cross sections on the order of barns. High purity was achieved by using a stacked-column technique. In this technique, a single column is made with two types of resin packed sequentially into the column support. For this experiment, the column consisted of a 3-mm $\times$ 50-mm column of cation-exchange resin (Bio-Rad AG-MP-50, 200-400 mesh) on top of a 3-mm $\times$ 10-mm column of anion-exchange resin (Bio-Rad AG 1-X8, 200-400 mesh).

For this procedure, the activity was transported via capillary about 80 meters to a collection site in the chemistry laboratory at the LBL 88-Inch Cyclotron. The activity and KCl were dissolved in 20 μL of 0.5 M HCl to which a known quantity of ^{241}Am ($t_{1/2}$ = 432 a) had been added as a yield tracer. The resulting solution was passed through the stacked column. Elution with concentrated HCl allowed americium to be separated from monovalent fission products, divalent fission products, and the lanthanides in the top portion (cation exchange) of the column, and then plutonium and neptunium were adsorbed by the bottom portion (anion exchange) of the column.

The fraction containing americium was collected, and americium was coprecipitated with CeF_3. The precipitate was filtered, washed, and then counted with an intrinsic-germanium γ-spectroscopy system. In the case of ^{232}Am, the final coprecipitation step was omitted to minimize the delay between the end of the irradiation and the start of the counting. The ^{232}Am was

then directly γ counted as a liquid sample. A flow chart of this separation procedure is shown in Figure 5. The total time required for this procedure was approximately four minutes if the coprecipitation was performed, or ninety seconds without it.

Fission from the respective εDF branches was measured on an alternating basis with the γ samples from the chemical separation. Samples for the fission measurements were produced by collecting the aerosols on a tantalum foil in the same collection apparatus as used in the chemical separations. The tantalum foil was flamed to red heat and counted in a windowless 2π gas flow proportional counter. The efficiency of this detector for fissions was determined to be 98.6% with a calibrated ^{252}Cf source.

By measuring the fission production rate and the EC decay on an alternating basis, any unknown values cancel out in the calculation of P_{DF} provided these values oscillate more slowly than the rate of the experiments (6-12 per hour). Therefore, values which would normally have to be estimated, such as gas-jet yield or effective target thickness, are time-averaged out of the calculation of P_{DF}. This increases the reliability of the measurement.

4.4 X-ray–Fission Correlation Procedure

The time correlation between the K-capture x-ray and the subsequent fission was measured using aerosols collected directly without any chemical separation. The aerosols were collected on a thin substrate for a suitable interval and the collector was placed before a light-tight transmission-mounted 300-mm^2 silicon surface barrier detector operated in air. In most experiments, the SSB detector and foil were sandwiched between two germanium γ detectors. In one measurement on ^{234}Am, a NaI(Tl) detector was added to provide better timing resolution.

Since fission produces about 10 prompt γ rays from the fission fragments [26, 34], a high overall γ-detection efficiency would reject many of the true

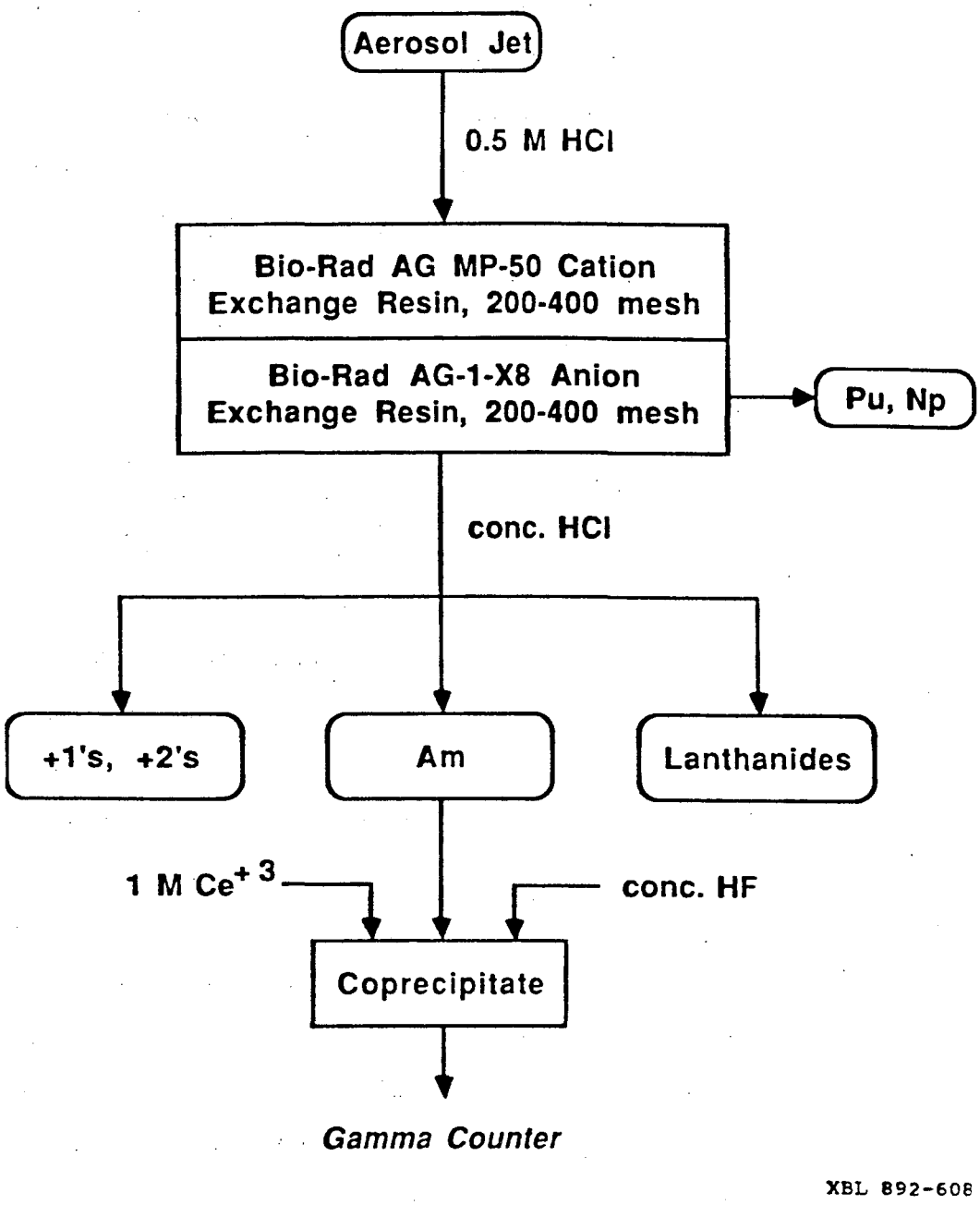

Figure 5: Flow chart of the procedure used to isolate americium from the ^{237}Np irradiations in a form suitable for γ counting.

x-ray events by summing the x-ray pulse with a pulse arising from prompt γ rays. On the other hand, if the overall γ efficiency is too low, the observed x-ray detection efficiency would be reduced, and hence the observed correlation rate would be reduced. By measuring the prompt γ rays from spontaneous fission in a source of ^{252}Cf, the spacing between the γ detectors and the sample was adjusted to bring the summing rejection level to 50%. As long as the γ multiplicity of the ^{234}Am εDF decay mode is not grossly different than that of ^{252}Cf, this would maximize the number of detected correlations. In the final configuration, each detector subtended a solid angle of about 6.7% of 4π. A 50% summing rejection level gives an overall correlation detection efficiency, using both germanium detectors, of 6.7% for each detected fission.

The signal from the SSB detector provided a common start for up to three electronic time-to-amplitude converters (TACs). The stop signals for the first and second TACs were provided by the first and second germanium γ detectors, respectively, and the stop signal for the third TAC (in the last measurement) was provided by the NaI(Tl) detector. The time window on the TACs was $\pm$500 ns. Calibrations were obtained using the prompt γ rays from the fission of ^{252}Cf and the γ rays in coincidence with the α particles from the decay of ^{249}Cf. The timing resolution of the germanium detectors was $\sim$12 ns full-width at half-maximum (FWHM), and the energy resolution of these detectors was $\sim$1.2 keV FWHM in the plutonium K x-ray region. The timing resolution of the NaI(Tl) detector was $\sim$3 ns FWHM, and its energy resolution was $\sim$30 keV FWHM in the 100-keV region.

5 Results and Discussion

5.1 Elemental Assignment

5.1.1 ^{232}Am

Using the chemical procedure described in **4.3.1**, 26 samples were processed and counted over about three hours. In each case, the aerosols were collected for three minutes and then subjected to the chemical separation. Each sample was counted continuously for approximately 18 minutes. Eleven fissions were observed in the americium fraction, and none were observed in the Np/Pu fraction.

Based on this distribution, the fission activity produced in the 99-MeV α irradiation of ^{237}Np was assigned to americium or delayed fission from an americium precursor.

5.1.2 ^{234}Am

38 samples were processed through the short chemistry and counted over about four hours. Again, the aerosols were collected for three minutes and the samples were counted for approximately 18 minutes. Twenty-seven fissions were observed in the americium fraction, and one was observed in the Np/Pu fraction. The one fission in the second fraction is consistent with the amount of americium expected to tail into this fraction. Prior tracer studies of this procedure had shown cross-contamination of each fraction to be about 2%. The 6.46-MeV α group attributed [35, 8] to ^{234}Am was also observed in the americium fraction.

Based on these results, we have assigned the fission activity produced by 72-MeV α particles on ^{237}Np to americium (or the delayed fission from an americium precursor).

5.2 Fission Properties

The εDF properties of ^{232}Am and ^{234}Am were measured using the **MG-RAGS** as described in **4.2**. The **MG** wheel was stepped at preset intervals so that the samples would spend approximately six half-lives between the six detector pairs. Each detector registered α particles and fissions for the full interval, except the first detector station. In the first station, signals from the α particles were suppressed for the first 12 seconds following the wheel motion to allow the ^{8}B+^{8}Li ($t_{1/2} < 1$ second) α activity produced from the beryllium in the target system to decay without causing excessive system deadtime. Fission signals from this detector were not seriously affected by these activities, and were analyzed for the full interval. After one full revolution of the wheel (80 positions), the wheel was replaced with a clean one so that any build-up of long-lived spontaneous fission activities was minimized.

The data were corrected for neutron emission using the method originated by Schmitt, Kiker, and Williams (SKW) [36]. The ^{252}Cf calibration parameters were taken from Weissenberger *et al.* [37]. The neutron emission function, $\overline{\nu}(A)$, was taken as similar to that of ^{252}Cf, normalized to $\overline{\nu}_T = 2.40$. This value was deduced from the systematics of$\overline{\nu}_T$ versus A.

5.2.1 Fission Properties

5.2.2 ^{232}Am

A total of 2201 coincident fission-fragment pairs was observed in these measurements using a wheel-stepping interval of 1.0 minute. From these events, the half-life was found to be 1.31 ± 0.04 minutes, closer to the early half-life of 1.4 ± 0.25 minutes reported by Skobelev [14] than the more recent value of 0.92 ± 0.12 minutes reported by Habs [15]. The decay curve for this fission activity is shown in Figure 6. Each point on the decay curve has been normalized to represent the same number of samples per detector station.

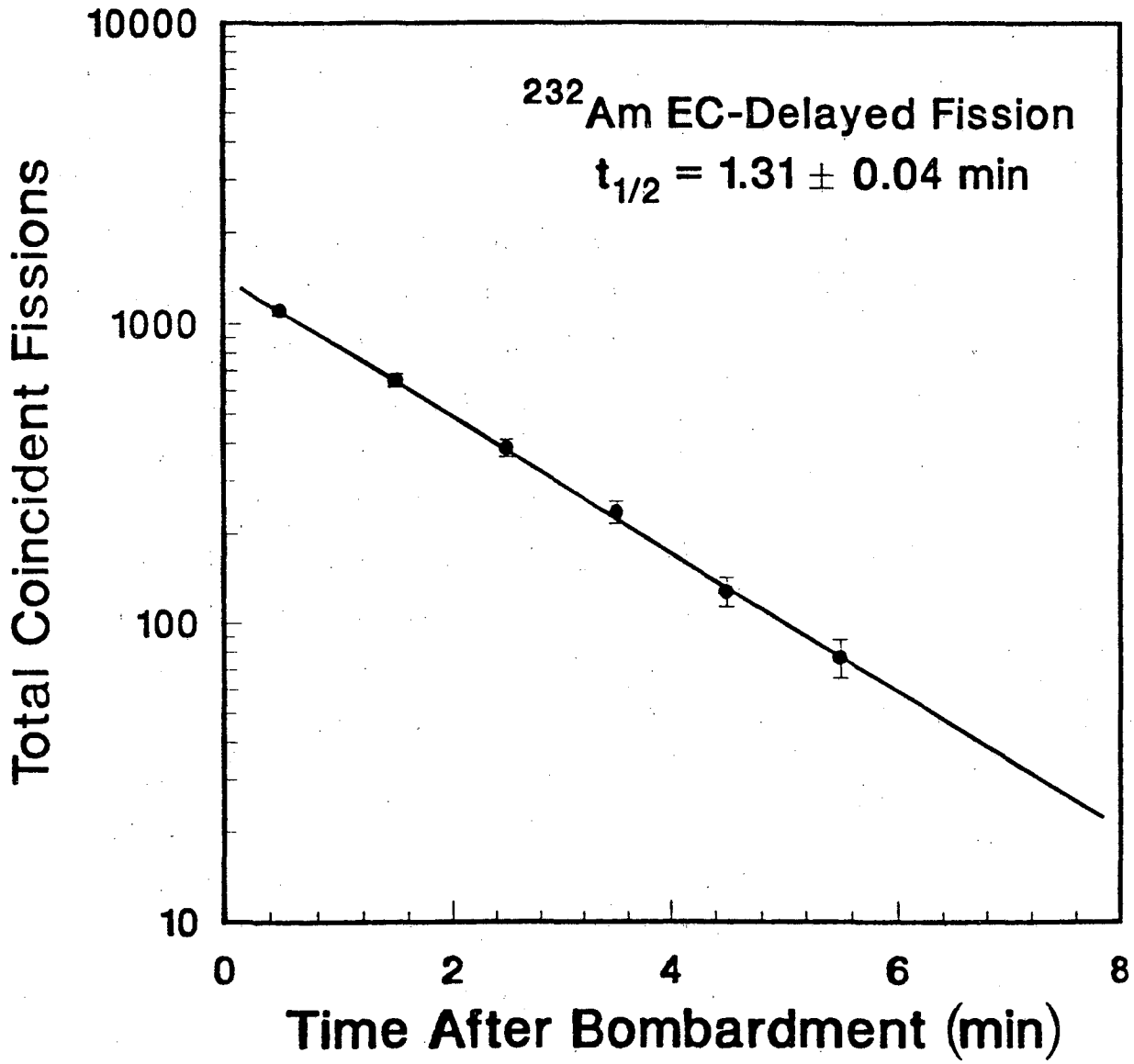

Figure 6: Decay curve of the ^{232}Am EC-delayed fission activity as measured on **MG-RAGS**. The wheel stepping time was 1.0 minute per station.

This is necessary since, for each wheel, the first station sees 80 foils before the acquisition is stopped while the second station sees 79, the third 78, and so on. The correction is fairly small (0% for the first station, rising to 12% for the last), but can significantly affect the measured half-life.

From the decay curve, an apparent fission cross section was estimated for the ^{232}Am εDF mode from this reaction. The effective target thickness was estimated by extrapolating low-energy recoil ranges for the compound nucleus linearly to zero energy. Recoil ranges were taken from Northcliffe and Schilling [38], and extrapolated when necessary. This method gave an estimate of the effective target thickness of 100 μg/cm^2 per target. The efficiency of the aerosol-transport system was taken as 100%, although it could be lower. These assumptions result in an apparent fission cross-section of about 2.5 nb.

Fission from ^{232}Am was observed to have a highly asymmetric mass distribution, with no trace of the thorium-anomaly. The mass-yield distribution is clearly two-humped, with a well-defined valley (after correction for neutron emission using the SKW [36] method with the constants of Weissenberger [37]) with no evidence of a symmetric component. The total kinetic energy distribution is symmetric about 174 $\pm$ 5 MeV with no evidence of multiple components. The TKE and mass-yield distributions are presented graphically in Figure 7.

The behavior of the TKE and $\overline{\text{TKE}}$ as a function of mass fraction is shown in the TKE contour [39] plot in Figure 8. The data in this figure suggest that the average TKE of the ^{232}Am εDF for symmetric mass division is about the same as it is for asymmetric division. This is unusual for low-energy fission of light actinides, and hints that shell effects in the fission fragments of ^{232}Pu are influencing its fission. $\overline{\text{TKE}}$ for the near-symmetric division is based on only 46 events, so the statistical significance of this behavior is small. The $\overline{\text{TKE}}$ value of 174 MeV for the ^{232}Am εDF is comparable to the predicted

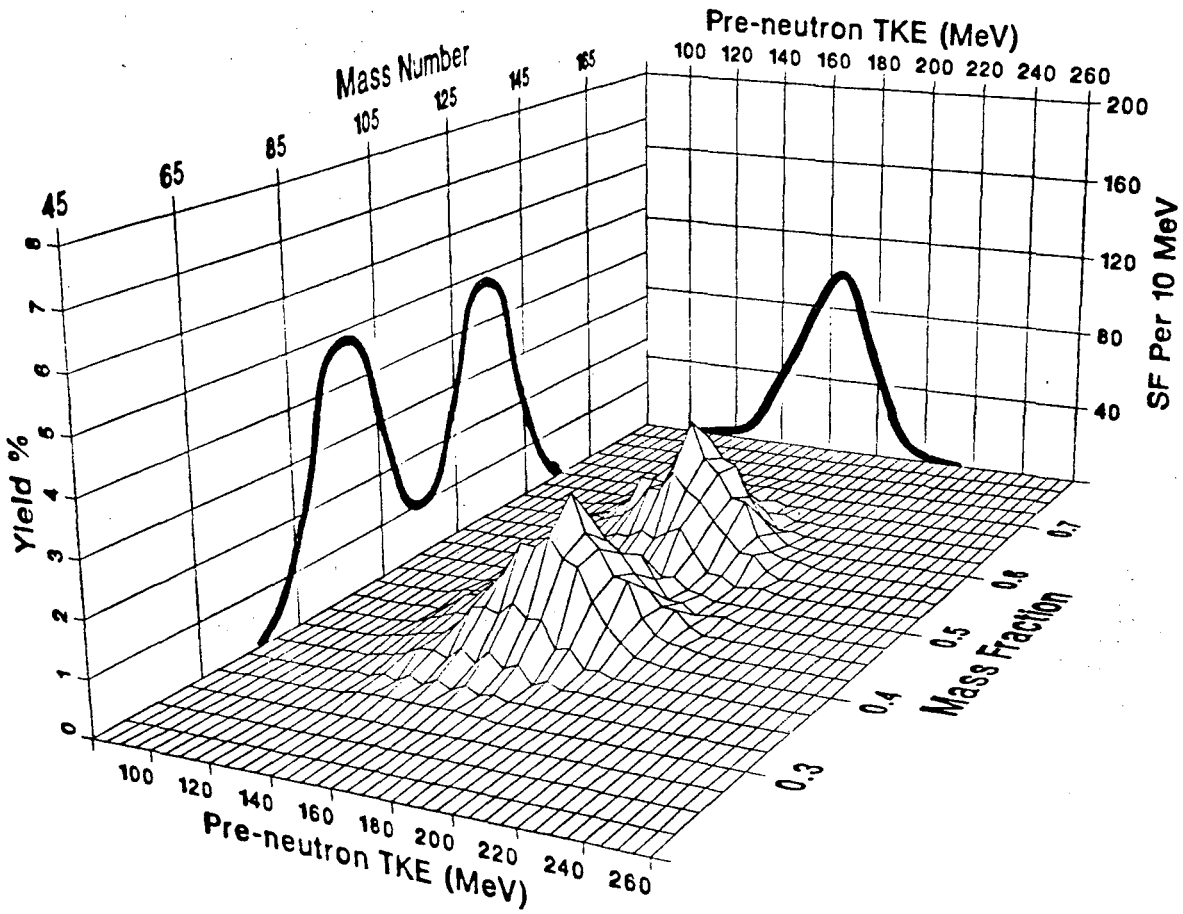

Figure 7: Pre-neutron emission total kinetic energy (TKE) distribution of the ^{232}Am εDF mode and pre-neutron emission mass-yield distribution.

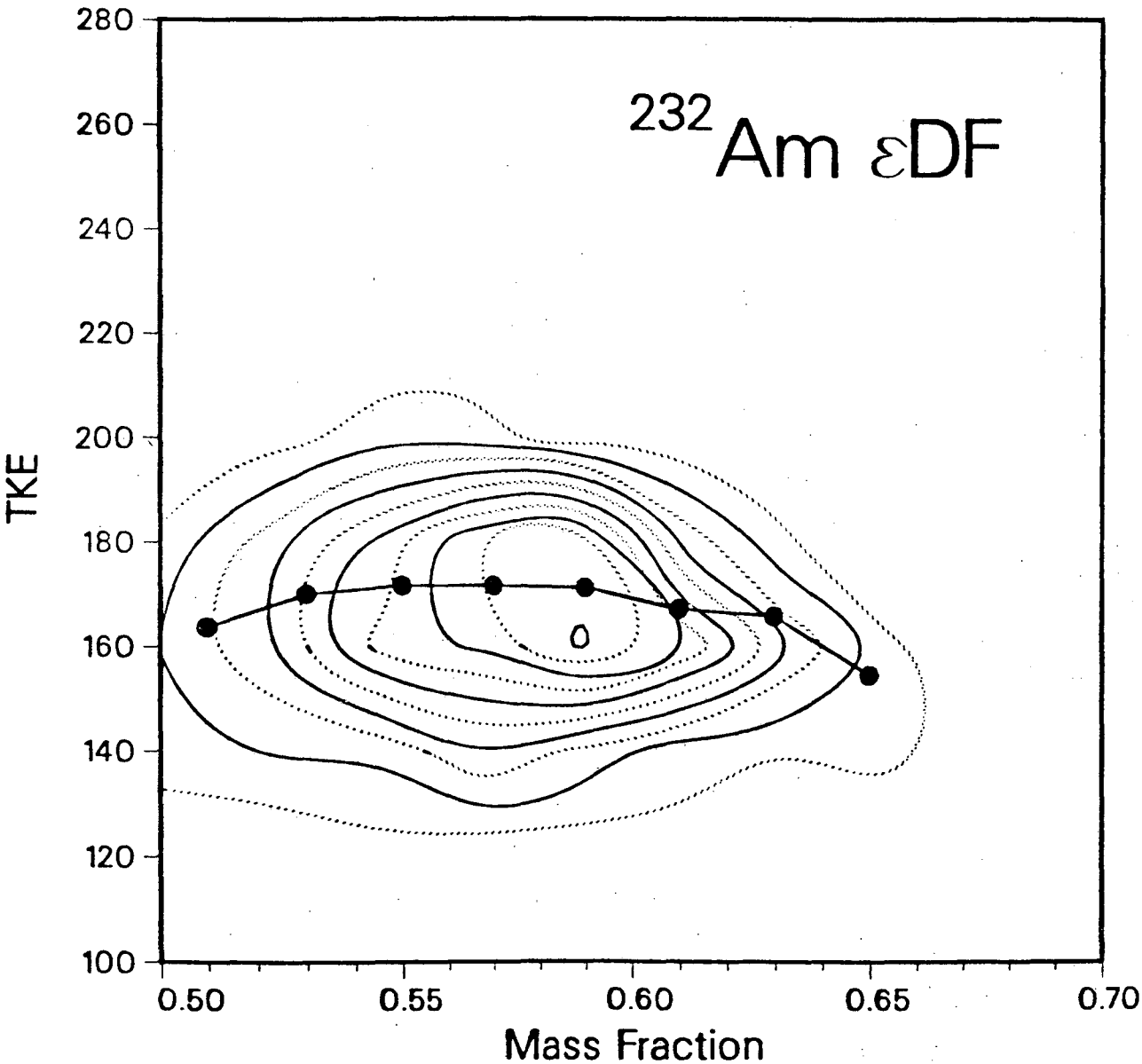

Figure 8: Total kinetic energy and average total kinetic energy of ^{232}Am as a function of mass fraction.

$\overline{\text{TKE}}$ [40, 41] for ground state fission from ^{234}Pu, as shown in Figure 9. The fission properties of the ^{232}Am εDF mode are summarized in Table 3.

5.2.3 ^{234}Am

A total of 1188 coincident fission-fragment pairs was observed in these measurements using a wheel-stepping interval of 2.50 minutes. From these events, a considerably more accurate value of the half-life was obtained than previously [11, 12, 14, 18] reported. The half-life was found to be 2.32 ± 0.08 minutes, slightly shorter than found in the previous reports (See Table 1). The decay curve for this fission activity is shown in Figure 10. Each point on the decay curve has again been normalized to represent the same number of samples per detector station.

From the decay curve, we can estimate an apparent fission cross section for the ^{234}Am εDF mode from this reaction. The effective target thickness was estimated (as before) to be 75 μg/cm^2 per target. The efficiency of the aerosol-transport system was again taken as 100%. These assumptions result in an apparent fission cross-section of about 0.2 nb.

Fission from ^{234}Am was also observed to have a highly asymmetric mass distribution. Pre- and post-neutron emission values are given in Table 3. Figure 11 shows the TKE and mass-yield distributions of the ^{234}Am εDF mode after corrections for neutron emission. The mass-yield distribution has a high peak-to-valley ratio, indicating highly asymmetric mass division. The TKE distribution is symmetric, and shows only one component. The behavior of the TKE and $\overline{\text{TKE}}$ as a function of mass fraction is shown in the TKE contour [39] plot in Figure 12. In this case, the $\overline{\text{TKE}}$ at symmetry dips, as expected for light actinides, but again the statistical significance of this point is poor (26 events). This, however, would be the expected behavior if a spherical subshell at N=66 is exerting a strong effect on the fission fragments of ^{232}. Since ^{234}Pu is two neutrons heavier, the symmetric fragments are

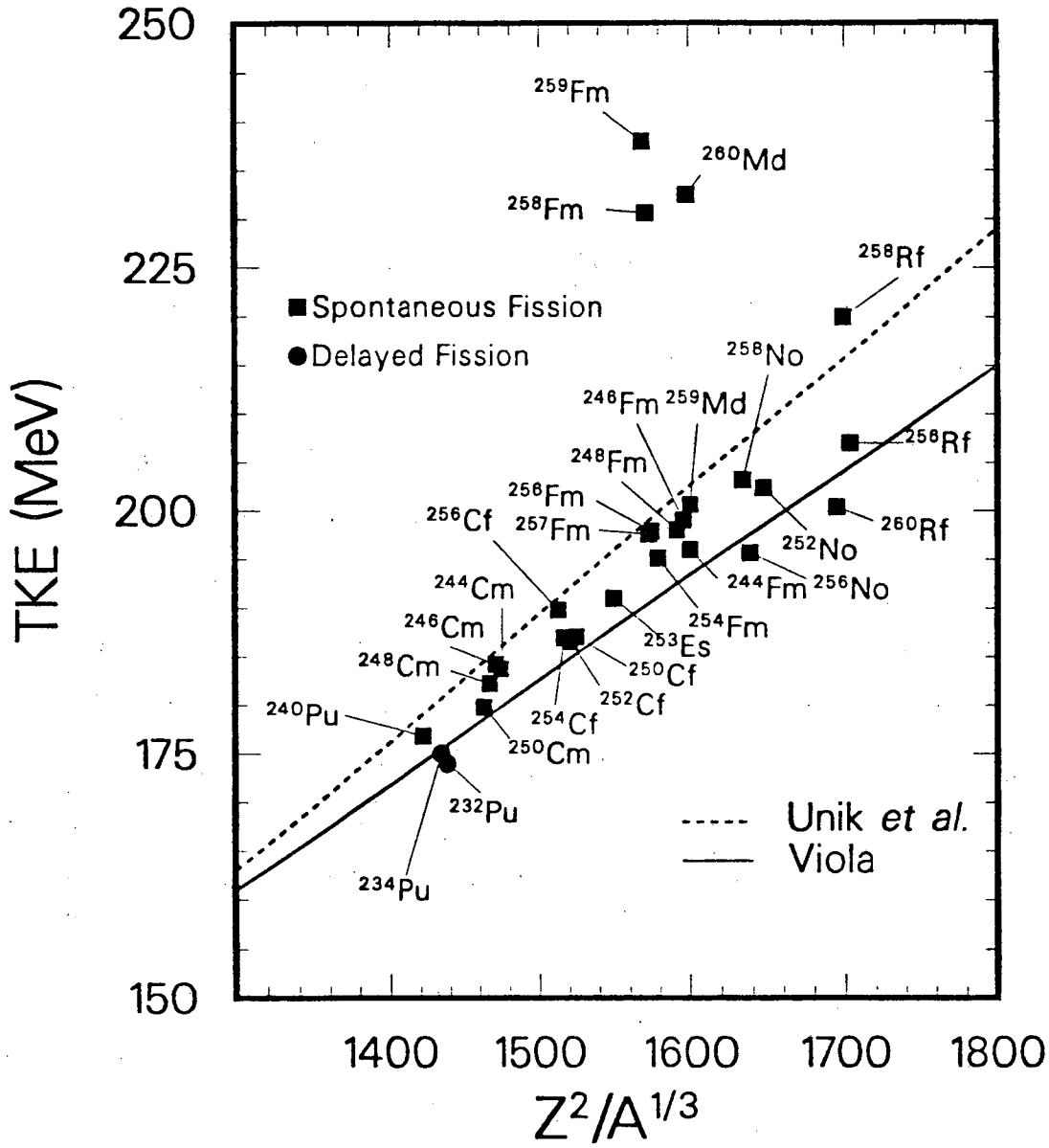

Figure 9: Average total kinetic energy as a function of $Z^2/A^{1/3}$. The solid line is a linear fit of Viola [40], and the dashed line is from Unik *et al.* [41]. Ground-state (spontaneous) fission data for the trans-berkelium actinides are taken from Hoffman and Somerville [34], and data for the lighter actinides are from Hoffman and Hoffman [26]. $Z^2/A^{1/3}$ for the americium delayed fission is calculated for the plutonium daughter, since that is the fissioning nucleus.

Table 3: Summary of the fission characteristics of the εDF mode of ^{232}Am and ^{234}Am.

	^{232}Am[a]	^{234}Am[a]
Post-neutron $\overline{\text{TKE}}$[b]	173 ± 5 MeV	174 ± 5 MeV
Pre-neutron $\overline{\text{TKE}}$	174 ± 5 MeV	175 ± 5 MeV
Post-neutron $\overline{\text{KE}}$[c] of high-energy fragment	99.4 ± 1.9 MeV	100.1 ± 2.0 MeV
Post-neutron $\overline{\text{KE}}$ of low-energy fragment	73.6 ± 2.0 MeV	73.5 ± 1.5 MeV
Pre-neutron $\overline{\text{KE}}$ of high-energy fragment	100.2 ± 1.9 MeV	101.2 ± 2.0 MeV
Pre-neutron $\overline{\text{KE}}$ of low-energy fragment	74.2 ± 2.0 MeV	74.1 ± 1.5 MeV
Average mass of the light fission fragment	98.7 ± 0.3	99.0 ± 0.1
Average mass of the heavy fission fragment	133.3 ± 0.3	135.0 ± 0.1
Assumed $\overline{\nu}_T$	2.4	2.4

[a]Calculated using the Schmitt, Kiker, and Williams (SKW) [36] method and Weissenberger [37] constants.
[b]Average total kinetic energy.
[c]Average kinetic energy.

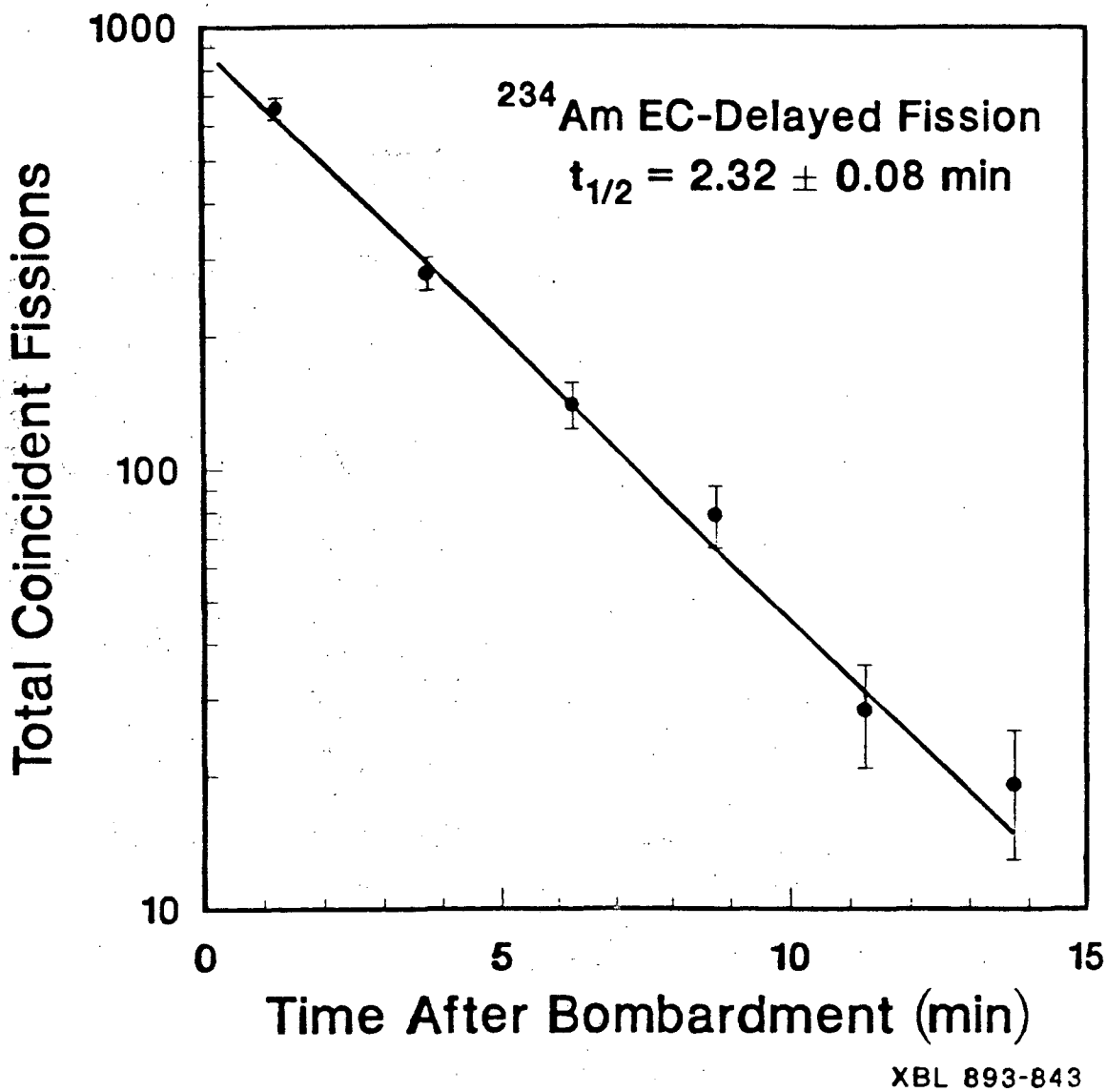

Figure 10: Decay curve of the ^{234}Am EC-delayed fission activity as measured on **MG-RAGS**. The wheel stepping time was 2.50 minutes.

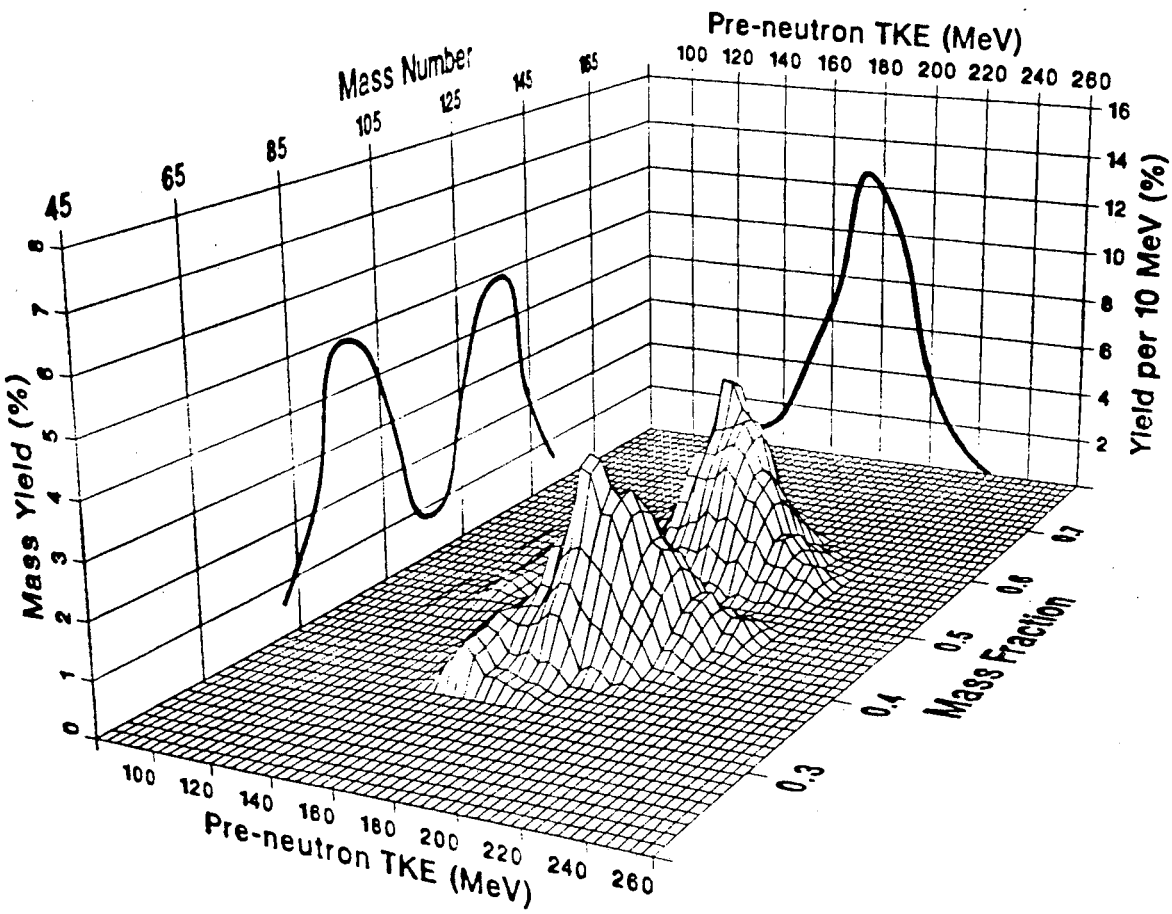

XBL 897-2684

Figure 11: Pre-neutron emission total kinetic energy (TKE) distribution of the ^{234}Am εDF mode and pre-neutron emission mass-yield distribution.

each further from the subshell. The $\overline{\text{TKE}}$ value of 175 MeV (SKW with Weissenberger constants) for the ^{234}Am εDF is comparable to the predicted $\overline{\text{TKE}}$ [40, 41] for ground state fission from ^{234}Pu, as shown in Figure 9. The fission properties of ^{234}Am εDF are summarized in Table 3.

5.3 P_{DF} and σ_ε Results

Americium fractions were repeatedly isolated chemically in order to measure the americium K-capture x-rays. Fission measurements were made on an alternating basis with the chemical separations. The chemically purified americium samples were γ counted repeatedly, and the fission samples were each counted in the proportional counter, and the integrated fissions were recorded. The γ spectra were analyzed using the **SAMPO** [42] computer code, and half-life analysis was performed with the **CLSQ** [43] code.

Major contaminants included ^{237}Am and ^{238}Am, probably produced by stripping reactions. A small amount of ^{7}Be, which was produced from the target backings, followed the americium, as did small amounts of ^{28,29}Al and ^{27}Mg. The aluminum and magnesium were most likely produced by scattered beam on the aluminum target-holder cards. Half-life analysis confirmed the assignment of these peaks.

The initial activities determined for the americium electron-capture decay mode were corrected for detector efficiency, chemical yield, branching ratio, and K-fluorescence yield (taken as 97.7% [44]). The resulting initial disintegration rates were used for the calculation of σ_ε and P_{DF}.

The electron-capture cross section was calculated based on the following assumptions. First, the target thickness was estimated the same way as for the apparent fission cross-section, yielding an effective total target thickness of 75 μg/cm^2 per target for ^{234}Am and 100 μg/cm^2 per target for ^{232}Am. Second, the gas-jet yield was assumed to be 100%. Third, because of the lack of discernible γ lines in the spectrum with half-lives consistent with

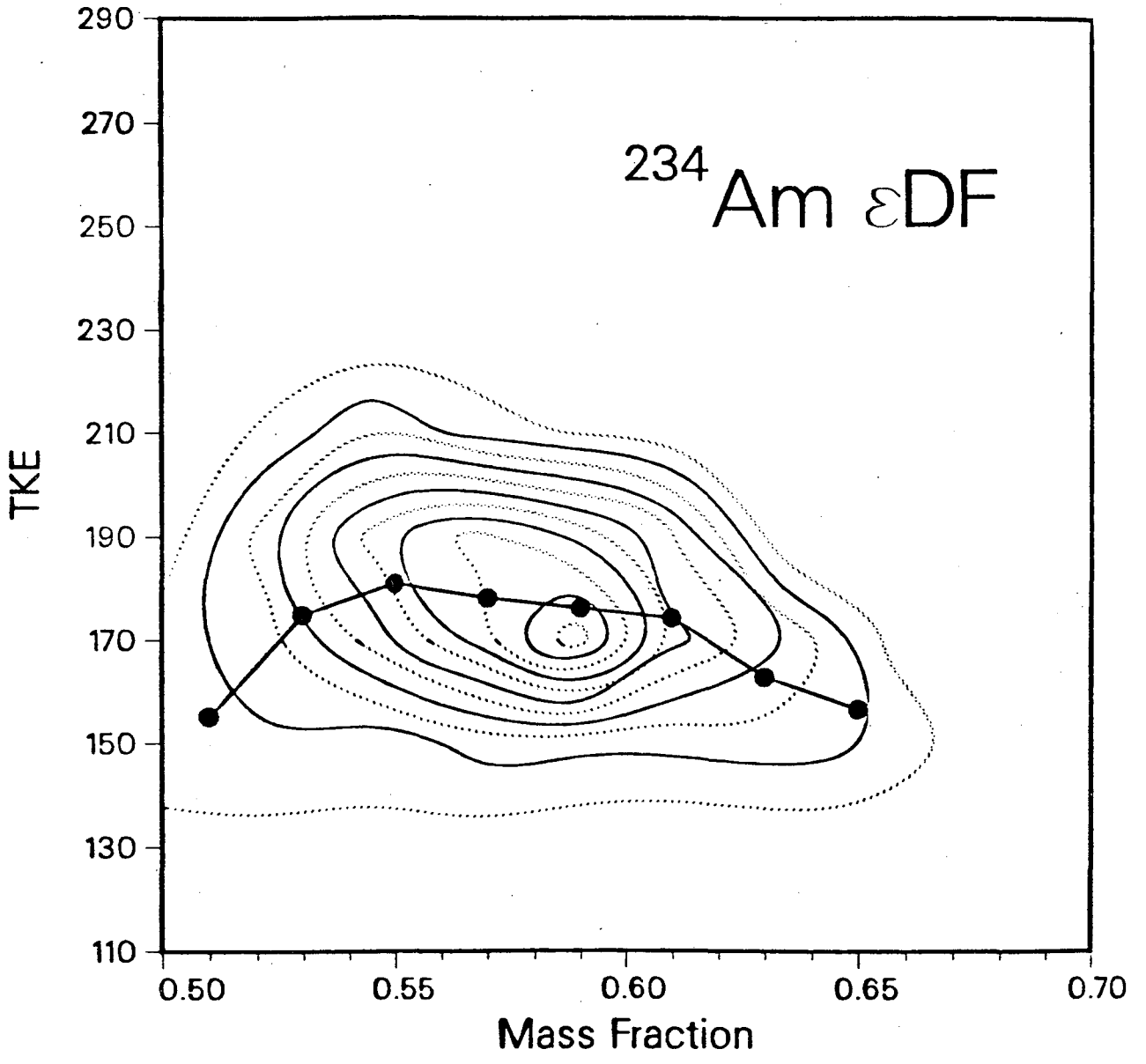

Figure 12: Total kinetic energy and average total kinetic energy of ^{234}Am as a function of mass fraction.

the decay of ^{232}Am or ^{234}Am, it was assumed that the level densities of the plutonium daughters were high enough that deexcitation proceeded through a series of high-energy (500-1000 keV) low-multipolarity transitions. Based on this assumption, the K x-ray production from internal conversion was taken as negligible. Of course, the last few transitions could be more highly converted, but without detailed information about the daughter level schemes any estimates on K-conversion would not be meaningful.

The delayed fission probability was calculated from the electron-capture initial activities and the number of fissions observed in the alternating fission samples. By measuring each quantity nearly simultaneously, experimental variables such as the target thickness, the beam flux (since our flux was held constant throughout this measurement, with less than 5% deviation), and the gas-jet yield should all cancel out. This allows us to calculate P_{DF} with a variant of Equation (1),

$$P_{DF} = \frac{\lambda I_f / [e^{-\lambda t_1} - e^{-\lambda(t_1+t_C)}]}{D_{0,\varepsilon}}, \tag{5}$$

where λ is the decay constant for ^{234}Am, I_f is the number of fissions observed in a counting time t_C, t_1 is the time from end of bombardment to the start of the fission counting, and $D_{0,\varepsilon}$ is the initial activity for electron capture. Employing this relationship, P_{DF} was calculated and an error-weighted average is reported, encompassing all of the separate determinations.

5.3.1 ^{232}Am

The K x-ray region from a representative γ spectrum is shown in Figure 13. The plutonium x-rays resulting from the electron capture of americium are weak, but visible. Half-life analysis of the Pu K x-rays revealed a two-component decay curve, with one component being consistent with 1.31 min, and the other on the order of an hour. The long component was a mixture of the ^{237}Am ($t_{1/2}$ = 73 min) and ^{238}Am ($t_{1/2}$ = 1.63 hr), and the short one was

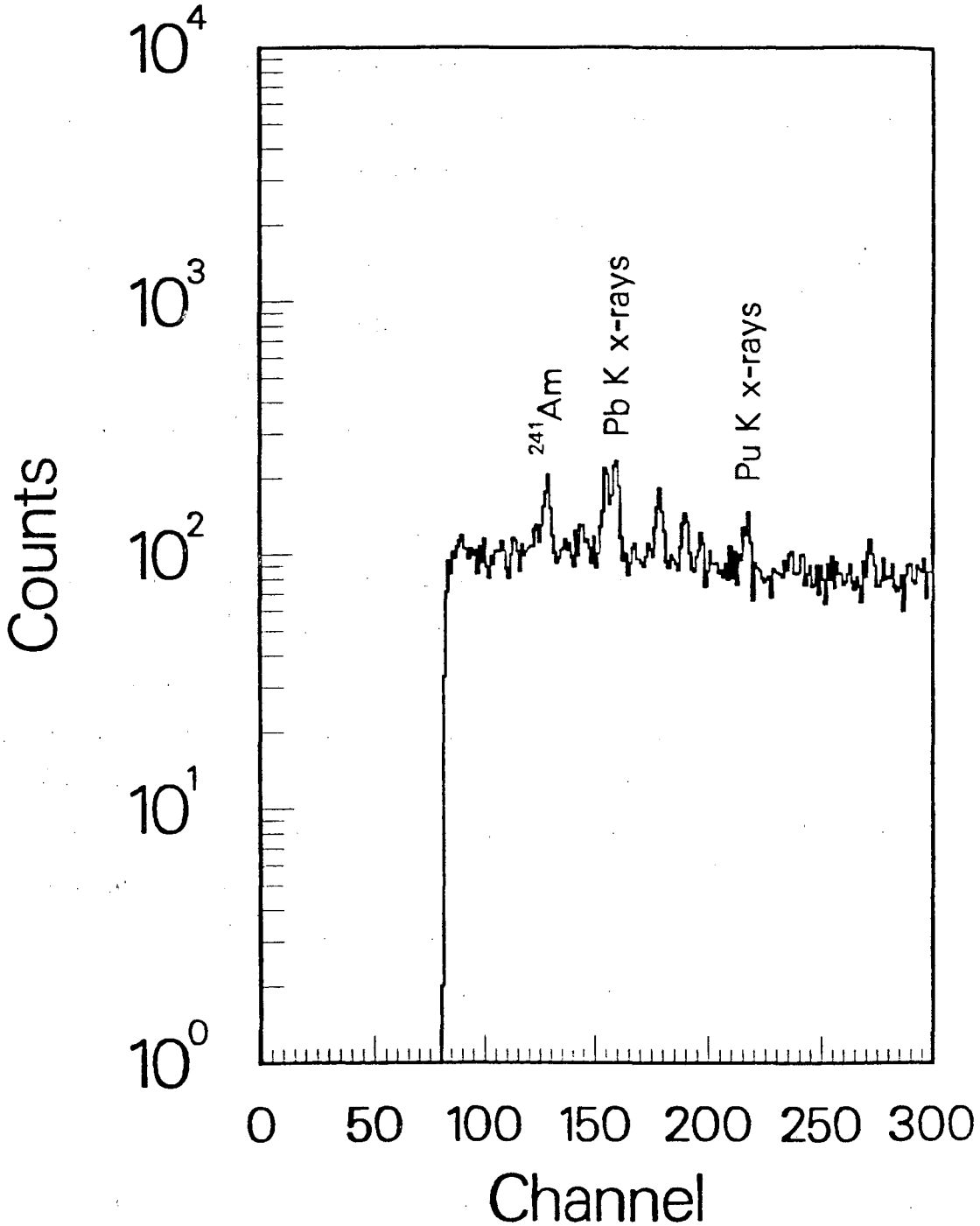

Figure 13: The K x-ray region of the gamma spectrum of a chemically purified ^{232}Am sample.

^{232}Am. The K x-rays were fitted with two components using **CLSQ**, with the short component set at 1.31 min and the long component allowed to vary to produce the best fit. An example of such a fit is shown in Figure 14.

The resulting initial count rates of the ^{232}Am electron-capture decay mode were converted to D_0 values for the calculation of P_{DF} by Equation (5). Employing this relationship and averaging over all of the separate determinations yielded a value of P_{DF} of $(6.9 \pm 1.0) \times 10^{-4}$ at the 1σ (68%) confidence level. From these D_0 values, σ_ε was also found to be 1.3 ± 0.2 μb at the 1σ confidence level.

This value for P_{DF} is approximately a factor of twenty smaller than the value reported by Habs *et al.* [15], and nearly a factor of a hundred smaller than the estimate of Kuznetsov [19]. However, their P_{DF} values rely on evaporation codes to estimate σ_ε whereas our measurement uses thirty separate determinations of σ_ε through the plutonium K x-rays. Of course, this method of measuring P_{DF} is sensitive to K-conversion of γ rays, but it would require 20 γ rays that are 100% converted *per electron capture* to account for the discrepancy. It seems much more likely that the evaporation codes become unreliable for predicting the magnitude of the cross section when such a large number of neutrons are evaporated (^{232}Am was formed by the ^{237}Np$(\alpha, 9n)$ reaction) in all of the above experiments.

5.3.2 ^{234}Am

The K x-ray region from a representative γ-ray spectrum is shown in Figure 15. The plutonium x-rays resulting from the electron capture of americium are clearly visible. The only other peaks in this region are lead K x-rays and the 59.5-keV γ ray from the ^{241}Am yield tracer.

Half-life analysis of the Pu K x-rays revealed a two-component decay curve, with one component being short (about 2-3 minutes), and the other on the order of an hour. The long component was a mixture of the ^{237}Am

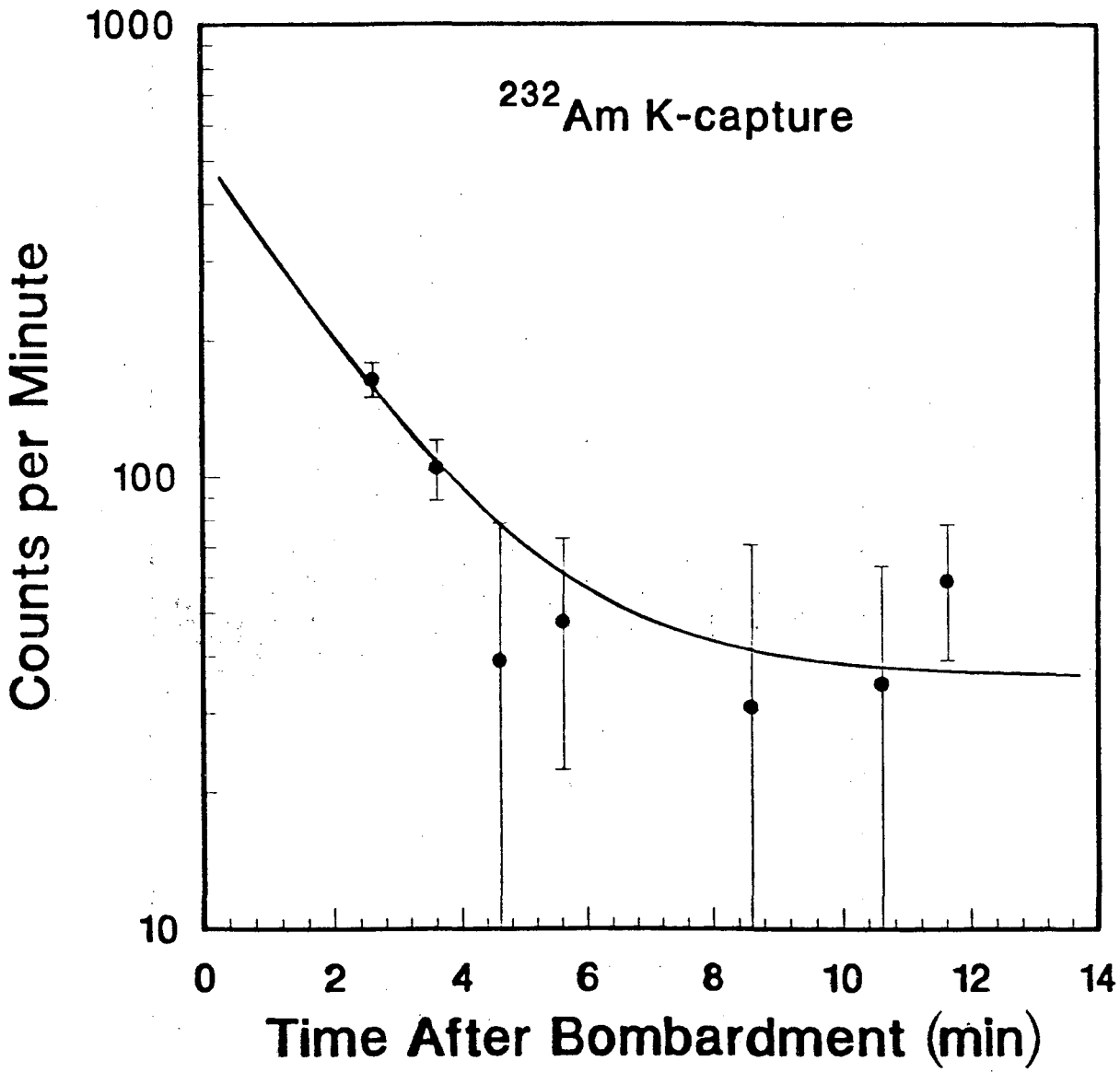

Figure 14: Representative half-life fit for the plutonium $K_{\alpha 1}$ x-ray observed in the chemically purified ^{232}Am sample.

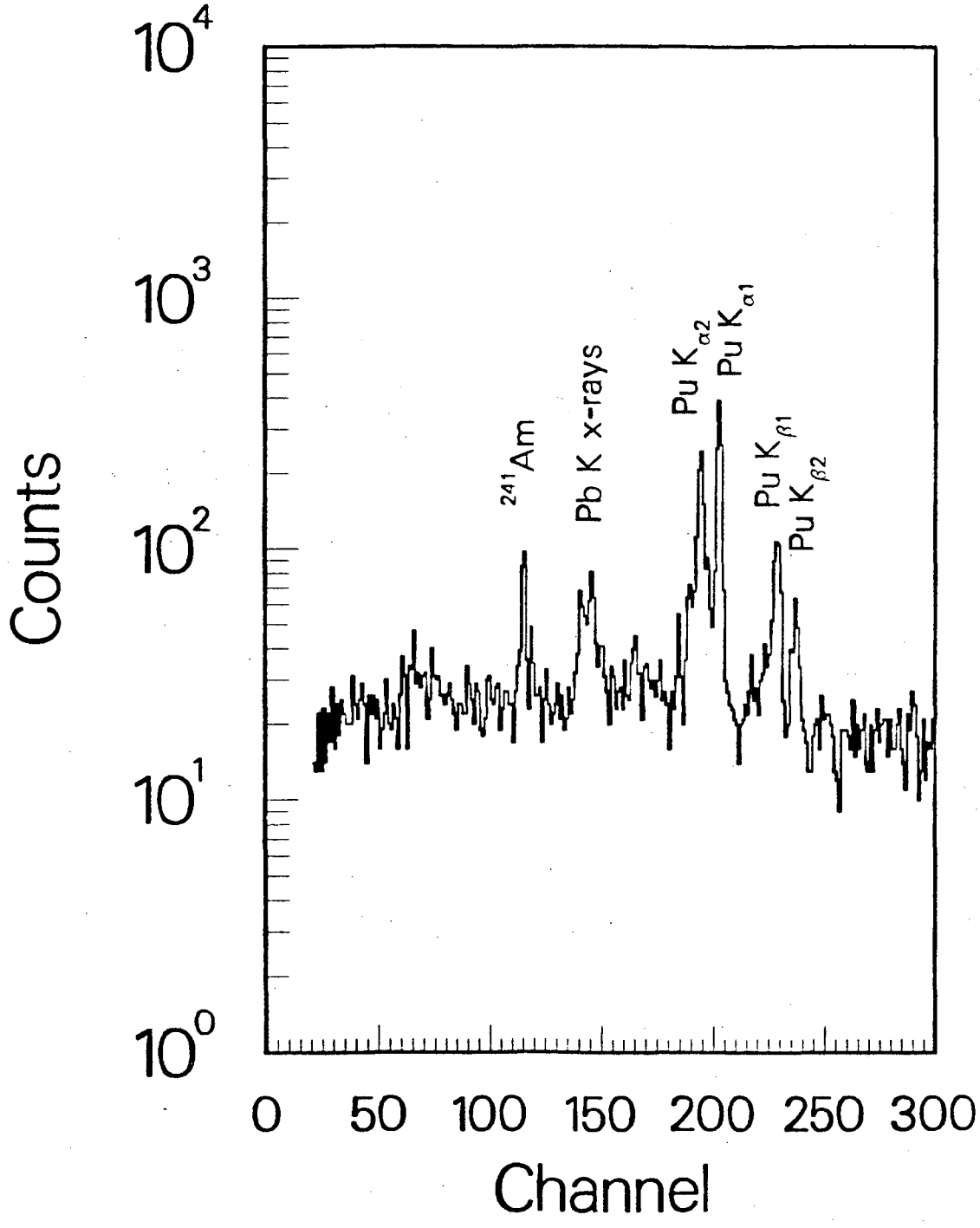

Figure 15: The K x-ray region of the gamma spectrum of a chemically purified ^{234}Am sample.

($t_{1/2}$ = 73 min) and ^{238}Am ($t_{1/2}$ = 1.63 hr), and the short was ^{234}Am. The K x-rays were fitted with two components using **CLSQ**, with the short component being set at 2.32 minutes and the long component allowed to vary. An example of such a fit is shown in Figure 16. The resulting initial disintegration rates were determined and used for the calculation of σ_ε and P_{DF}.

The electron capture cross section, σ_ε, was found to be 5.4 ± 1.3 μb at the 1σ (68%) confidence level. P_{DF} was calculated and averaged over all of the separate determinations. This yielded a value of P_{DF} of $(6.6 \pm 1.8) \times 10^{-5}$ at the 1σ (68%) confidence level. This value is consistent with the value predicted by Kuznetsov [19], and indicates that the region of unreliability in the evaporation codes are likely to begin after the $7n$ reaction, but before the $9n$.

5.4 X-ray–Fission Results

Samples were collected from the gas-jet system every four minutes for ^{234}Am and at two-minute intervals for ^{232}Am, and then these samples were placed in the counting chamber for the correlation studies. Figures 17(A) and 18(A) show the x-ray and γ spectrum of those events in prompt coincidence with the fission signal. The data in Figures 17(C) and 18(C) are the logarithms of a maximum-likelihood fit [8] L of an idealized x-ray spectrum (shown in Figure 18(B)) to the observed data as a function of the $K_{\alpha 1}$ position.

From the likelihood functions, the most probable $K_{\alpha 1}$ energies were found to be 103.8 ± 0.3 keV and 103.6 ± 0.5 keV for ^{232}Am and ^{234}Am, respectively, in excellent agreement with the plutonium $K_{\alpha 1}$ energy of 103.76 keV. The total number of K x-rays was found to be 42 ± 8 for ^{232}Am and 32 ± 6 for ^{234}Am by allowing the intensity of the ideal spectrum to vary within the maximum-likelihood analysis. Observed and expected x-ray intensities are given in Table 4.

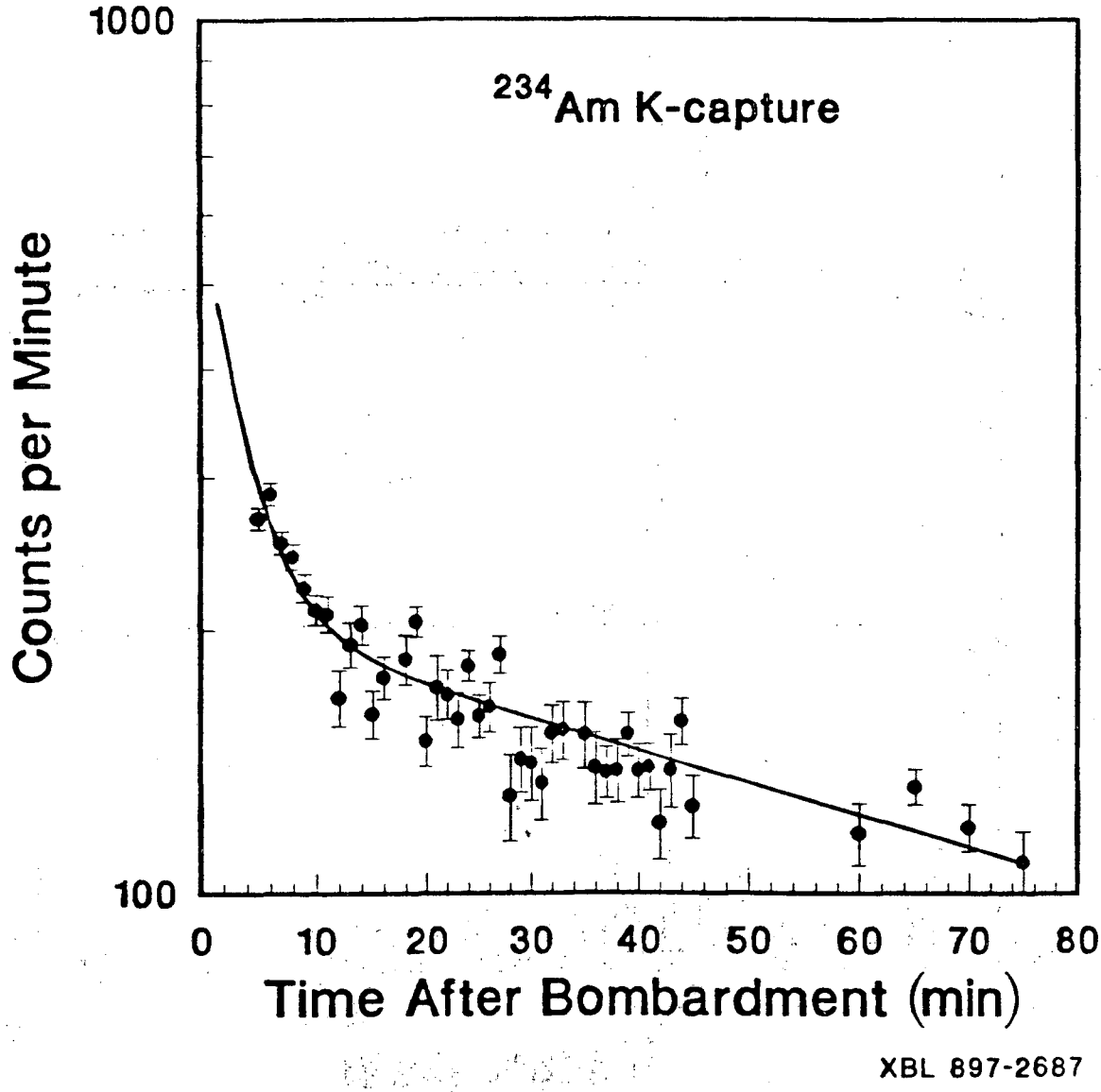

Figure 16: Half-life fit for the plutonium K x-rays observed from the chemically purified ^{234}Am sample.

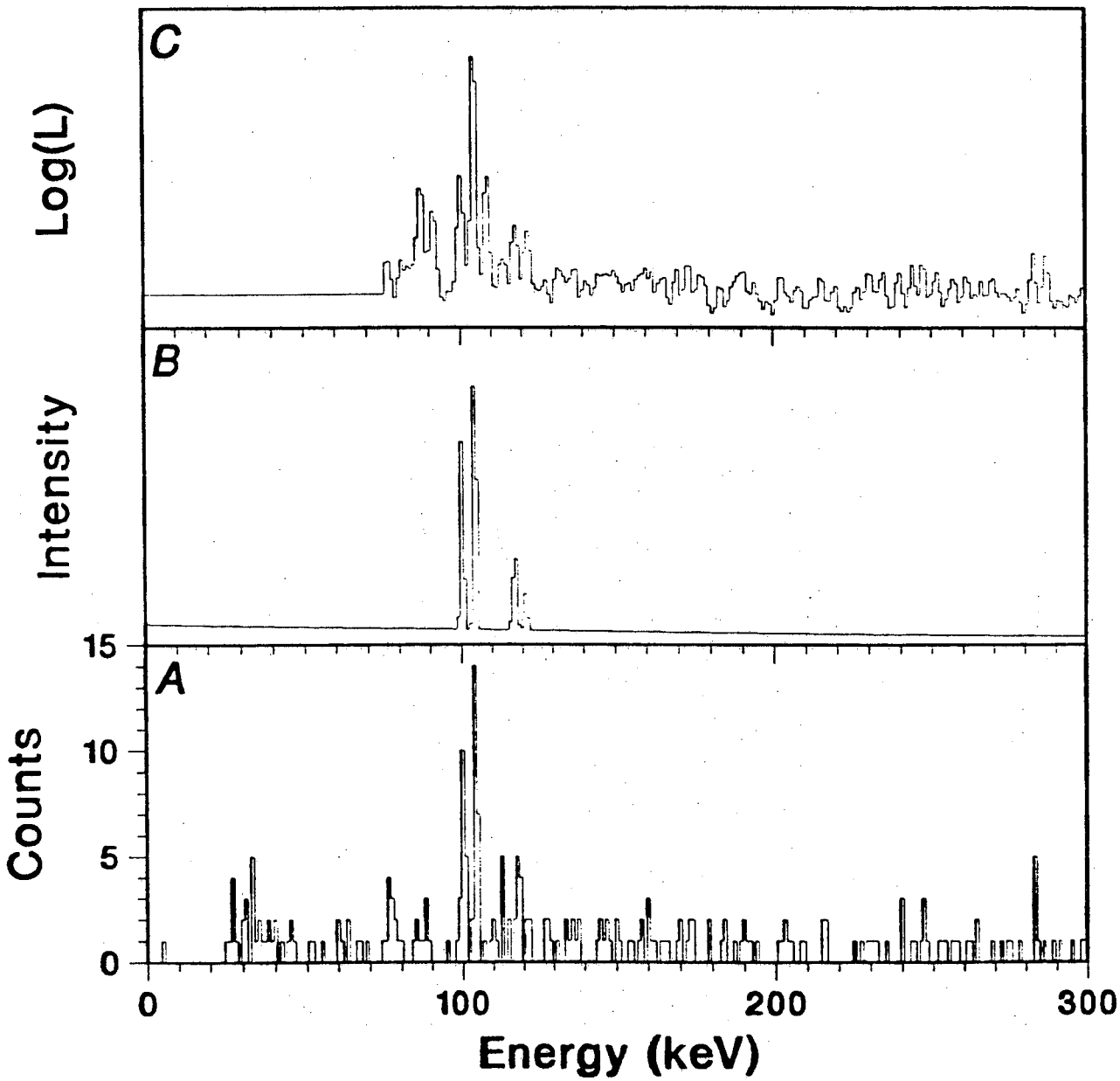

Figure 17: X-ray–fission correlation results for ^{232}Am. *A*: X-rays and γ rays in coincidence with delayed fission from ^{232}Am. *B*: An idealized plutonium K x-ray spectrum, based on the measured detector resolution and prompt γ-ray continuum. *C*: The likelihood function for the position of the ideal spectrum (*B*) in the data (*A*), as a function of the $K_{\alpha 1}$ position.

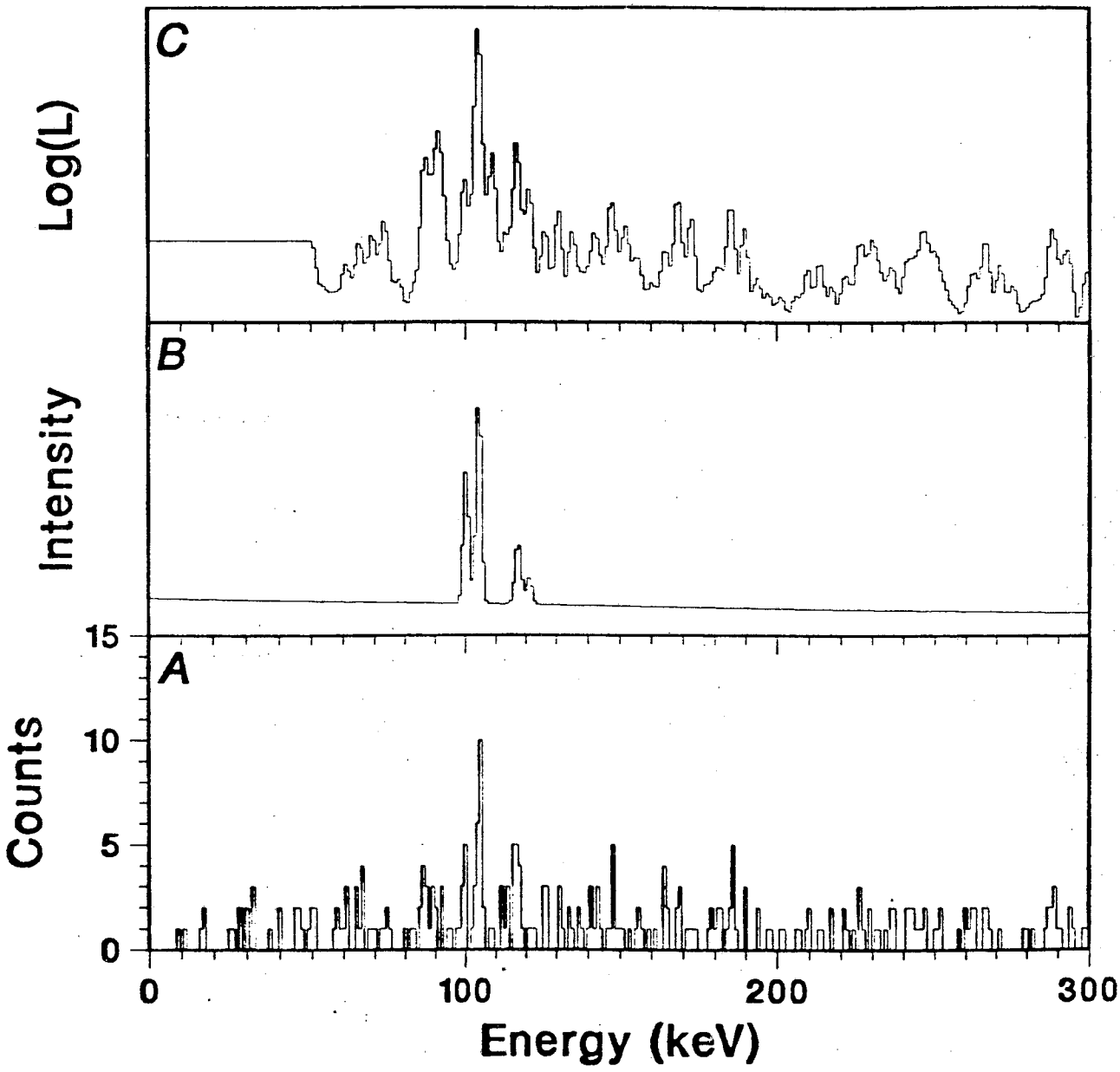

Figure 18: X-ray–fission correlation results for ^{234}Am. *A*: X-rays and γ rays in coincidence with delayed fission from ^{234}Am. *B*: An idealized plutonium K x-ray spectrum, based on the measured detector resolution and prompt γ-ray continuum. *C*: The likelihood function for the position of the ideal spectrum (*B*) in the data (*A*), as a function of the $K_{\alpha 1}$ position.

Table 4: Observed and expected x-ray intensities from the correlated x-ray–fission data. Expected x-ray intensities are taken from the **Table of Isotopes**. [44].

X-ray	E/keV	I_{theo}	No. Observed[a]	I_{obs}
^{232}Am:				
Pu $K_{\alpha 2}$	99.55	0.299	19	0.33 ± 0.09
Pu $K_{\alpha 1}$	103.76	0.479	23	0.40 ± 0.10
Pu $K_{\beta 1'}$	116.9	0.162	11	0.19 ± 0.06
Pu $K_{\beta 2'}$	120.6	0.060	4	0.07 ± 0.04
^{234}Am:				
Pu $K_{\alpha 2}$	99.55	0.299	10	0.20 ± 0.07
Pu $K_{\alpha 1}$	103.76	0.479	22	0.45 ± 0.12
Pu $K_{\beta 1'}$	116.9	0.162	14	0.29 ± 0.09
Pu $K_{\beta 2'}$	120.6	0.060	3	0.06 ± 0.04

[a] Approximately 15 ± 4 of the observed events are attributable to the prompt γ-ray continuum for the ^{232}Am study, and about 18 ± 5 for ^{234}Am.

No evidence was observed for fission delay times longer than the best timing resolution of these experiments, about 3-8 ns. The fact that plutonium x-rays can be seen requires that the lifetime of the fissioning state be longer than the time it takes the orbital electrons to fill a K-vacancy. The time required for this is on the order of 10^{-17} seconds [45]. We can therefore set boundaries on the excited states half-lives of 10^{-8} ns $< t_{\frac{1}{2}} < 3$ ns for both ^{232}Pu and ^{234}Pu. If the nucleus is truly 100% damped in the second well (as is commonly [7, 8, 15] assumed), then these limits are also limits on the lifetimes of the shape isomers ^{232f}Pu and ^{234f}Pu. These limits are consistent with the half-life systematics of plutonium shape isomers (See Figure 3 of Ref. [46]), from which one would expect the half-life of ^{234f}Pu to be in the range of 1 to 100 picoseconds, with ^{232f}Am being even shorter.

If the nucleus is strongly damped in the second well, then the coincidence γ-fission data provides a unique opportunity to study the level structure of the second well [47]. The highly specific coincidence requirement, along with the lack of structure in the fission prompt γ ray emission, would allow detection of γ transitions between levels in the second well (provided, of course, that the second well is at least partially populated by states above the lowest state in the well). For example, Figure 18 tantalizingly shows what appear to be true peaks at about 112, 147, 168, 185, 287 keV, and possibly others. With better statistics in the data and the addition of a γ-γ coincidence gate, it might be possible to construct a fairly complete level scheme for this shape isomer.

However, to study the level structure of the of the second well efficiently, it will be necessary to use a multiple-detector array such as **HERA** [48] or the proposed **GAMMASPHERE** [49]. A multiple-detector array is required to cover a large fraction of 4π with each individual detector subtending approximately 1% of 4π to overcome problems created by the high prompt γ-ray multiplicity intrinsic to fission. With an average γ multiplicity of 10, a

single detector which subtends 10% of 4π would have an effective correlation detection rate of 0% due to the 100% summing rejection level.

6 CONCLUSIONS

Light americium isotopes were produced using multiple ^{237}Np targets irradiated with α particles. The half-lives of ^{232}Am and ^{234}Am were determined to be 1.31 ± 0.04 minutes and 2.32 ± 0.08 minutes, respectively, using a rotating-wheel system. The fission properties of the εDF mode in ^{232}Am and ^{234}Am were measured. These are the first delayed-fissile nuclei for which measurements of the fission properties have been made. These are also the first nuclei for which both the fission and the EC branch leading to the fission have been directly measured.

The highly asymmetric mass-division and symmetric TKE distributions for both ^{232}Am and ^{234}Am show no trace of the thorium anomaly. Therefore, the transition region between "normal" double-humped mass distributions and the triple-humped distribution of the thorium anomaly must begin with lighter elements for this neutron number. Unfortunately, the lighter isotones have considerably smaller Q_ε values. This may reduce εDF in those nuclei to a level too low to measure their fission properties.

The εDF mode provides a mechanism for studying the fission properties of a nucleus far from stability near its ground state. No other technique currently exists which allows the study of near ground-state fission from a specific nucleus this far from β-stability.

Finally, the coincidence data between the plutonium x-ray and the fission provides direct proof that the fissions observed in this experiment are the result K-capture in americium followed by fission of excited states in the daughter plutonium nucleus. These data also provide the intriguing prospect of studying the level structure of the daughter shape isomers, which are not

attainable by other techniques.

7 ACKNOWLEDGEMENTS

This work was supported in part by the Director, Office of Energy Research, Division of Nuclear Physics of the Office of High Energy and Nuclear Physics of the U.S. Department of Energy under Contract DE-AC03-76SF00098.

The authors wish to thank the staff and crew of the LBL 88-Inch Cyclotron for their assistance.

References

[1] E. M. Burbidge, G. R. Burbidge, W. A. Fowler, and F. Hoyle, *Rev. Mod. Phys. 29*, 547 (1957).

[2] C.-O. Wene and S. A. E. Johansson, *Phys. Scripta 10A*, 156 (1974).

[3] C.-O. Wene, *Astron. & Astrophys. 44*, 233 (1975).

[4] H. V. Klapdor, T. Oda, J. Metzinger, W. Hillebrandt, and F. K. Thielman, *Z. Physik A 299*, 213 (1981).

[5] B. S. Meyer, W. M. Howard, G. J. Matthews, K. Takahashi, P. Möller, and G. Leander, *Phys. Rev. C 39*, 1876 (1989).

[6] Yu. A. Lazarev, Yu. Ts. Oganessian, and V. I. Kuznetsov, *Joint Institutes for Nuclear Research, Dubna, Report No. JINR-E7-80-719* (1980).

[7] Yu. P. Gangrskiĭ, M. B. Miller, L. V. Mikhaĭlov, and I. F. Kharisov, *Yad. Fiz. 31*, 306 (1980) [*Sov. J. Nucl. Phys. 31*, 162 (1980)].

[8] H. L. Hall, K. E. Gregorich, R. A. Henderson, C. M. Gannett, R. B. Chadwick, J. D. Leyba, K. R. Czerwinski, B. Kadkhodayan, S. A. Kreek, D. M. Lee, M. J. Nurmia, D. C. Hoffman, C. E. A. Palmer, and P. A. Baisden, submitted to *Phys. Rev. C.*

[9] H. V. Klapdor, C.-O. Wene, I. N. Isosimov, and Yu. W. Naumow, *Z. Physik A 292*, 249 (1979).

[10] H. L. Hall, K. E. Gregorich, R. A. Henderson, D. M. Lee, D. C. Hoffman, M. E. Bunker, M. M. Fowler, P. Lysaght, J. W. Starner, and J. B. Wilhelmy, *Phys. Rev. C 39*, 1866 (1989).

[11] V. I. Kuznetsov, N. K. Skobelev, and G. N. Flerov, *Yad. Fiz. 4*, 279 (1966) [*Sov. J. Nucl. Phys. 4*, 202 (1967)].

[12] V. I. Kuznetsov, N. K. Skobelev, and G. N. Flerov, *Yad. Fiz. 5*, 271 (1967) [*Sov. J. Nucl. Phys. 5*, 191 (1967)].

[13] É. E. Berlovich and Yu. P. Novikov, *Dok. Akad. Nauk SSSR 185*, 1025 (1969) [*Sov. Physics—Doklady 14*, 349 (1969)].

[14] N. K. Skobelev, *Yad. Fiz. 15*, 444 (1972) [*Sov. J. Nucl. Phys. 15*, 249 (1972)].

[15] D. Habs, H. Klewe–Nebenius, V. Metag, B. Neumann, and H. J. Specht, *Z. Physik A 285*, 53 (1978).

[16] R. Hingman, W. Kuehn, V. Metag, R. Novotny, A. Ruckelshausen, H. Stroeher, F. Hessberger, S. Hofmann, G. Muenzenberger, and W. Reisdorf, *Gessellschaft für Schwerionenforschung, Darmstadt, Report No. GSI 85-1*, 88 (1985).

[17] Yu. A. Lazarev, Yu. Ts. Oganessian, I. V. Shirokovsky, S. P. Tretyakova, V. K. Utyonkov, and G. V. Buklanov, *Europhys. Lett. 4*, 893 (1987).

[18] L. P. Somerville, A. Ghiorso, M. J. Nurmia, and G. T. Seaborg, *Lawrence Berkeley Laboratory Nuclear Science Division Annual Report, 1976-1977, Report No. LBL-6575*, 39 (1977).

[19] V. I. Kuznetsov, *Yad. Fiz. 30*, 321 (1979) [*Sov. J. Nucl. Phys. 30*, 166 (1979)].

[20] R. W. Hoff, *in* **Weak and Electromagnetic Interactions in Nuclei**, H. V. Klapdor, ed. (Springer-Verlag, Heidelburg, 1986), 207.

[21] R. W. Hoff, *Inst. Phys. Conf. Ser. No. 88/J. Phys. G: Nucl. Phys. 14 Suppl.*, S343 (1986).

[22] Yu. P. Gangrskiĭ, G. M. Marinescu, M. B. Miller, V. N. Samoyusk, and I. F. Kharisov, *Yad. Fiz. 27*, 894 (1978) [*Sov. J. Nucl. Phys. 27*, 475 (1978)].

[23] A. Baas–May, J. V. Kratz, and N. Trautmann, *Z. Physik A 322*, 457 (1985).

[24] P. Möller, W. D. Myers, W. J. Świątecki, and J. Treiner, *At. Data Nucl. Data Tables 39*, 225 (1988).

[25] H. L. Hall, M. J. Nurmia, D. C. Hoffman, *Nucl. Inst. Meth. A276*, 649 (1989).

[26] D. C. Hoffman and M. M. Hoffman, *Ann. Rev. Nucl. Sci. 24*, 151 (1974).

[27] H. J. Specht, *Rev. Mod. Phys. 46*, 773 (1974).

[28] H. J. Specht, *Phys. Scripta 10A*, 21 (1974).

[29] R. Vandenbosch and J. R. Huizenga, **Nuclear Fission**, (Academic Press, New York, 1973).

[30] E. Konecny, H. J. Sprecht, and J. Weber, *Phys. Lett. 45B*, 329 (1973).

[31] J. Blons, C. Mazur, D. Paya, M. Ribrag, and H. Weigmann, *Nucl. Phys. A414*, 1 (1984).

[32] M. G. Itkis, V. N. Okolovich, and A. Ya. Rusanov, *Fiz. Elem. Chastits At. Yadra 19*, 701 (1988) [*Sov. J. Part. Nucl. 19*, 301 (1988)].

[33] B. S. Bhandari and A. S. Al-Kharam, *Phys. Rev. C 39*, 917 (1989).

[34] D. C. Hoffman and L. P. Somerville, *in* **Charged Particle Emission from Nuclei Vol. III**, D. N. Poenaru and M. Ivaşcu, eds., (CRC Press, Boca Raton, Fla., 1989) 1.

[35] Y. A. Ellis-Akovali, *Nucl. Data Sheets 40*, 523 (1983).

[36] H. W. Schmitt, W. E. Kiker, and C. W. Williams, *Phys. Rev. 137*, B837 (1965).

[37] E. Weissenberger, P. Geltenbort, A. Oed, F. Gönnenwein, and H. Faust, Nucl. Inst. Meth. A248, 506 (1986).

[38] L. C. Northcliffe and R. F. Schilling, *Nucl. Data Tables A7*, 233 (1970).

[39] R. Brandt, S. G. Thompson, R. C. Gatti, and L. Phillips, *Phys. Rev. 131*, 2617 (1963).

[40] V. Viola, *Nucl. Data, Sect. B 1*, 391 (1966).

[41] J. P. Unik, J. E. Gindler, L. E. Glendenin, K. F. Flynn, A. Gorski, and R. K. Sjoblom, *in* **Proceedings of the 3rd IAEA Symposium on the Physics and Chemistry of Fission, 1973, Vol. 2** (International Atomic Energy Agency, Vienna, 1974), 19.

[42] J. T. Routti and S. G. Prussin, *Nucl. Inst. Meth. 72*, 125 (1969).

[43] J. B. Cumming, *NAS-NS 3107*, 25 (1963). Also, *Brookhaven National Laboratory Report No. BNL-6470* (1963).

[44] C. M. Lederer, V. M. Shirley, E. Browne, J. M. Dairiki, R. E. Doebler, A. A. Shihab-Eldin, L. J. Jardine, J. K. Tuli, and A. B. Buyrn, **Table of Isotopes, 7th Ed.** (John Wiley & Sons, New York, 1978).

[45] J. H. Scofield, *At. Data Nucl. Data Tables 14*, 121 (1974)

[46] D. N. Poenaru, M. S. Ivaşcu, and D. Mazilu, *in* **Charged Particle Emission from Nuclei Vol. III**, D. N. Poenaru and M. Ivaşcu, eds., (CRC Press, Boca Raton, Fla., 1989) 41.

[47] H. L. Hall, K. E. Gregorich, R. A. Henderson, C. M. Gannett, R. B. Chadwick, J. D. Leyba, K. R. Czerwinski, B. Kadkhodayan, S. A. Kreek, D. M. Lee, M. J. Nurmia, and D. C. Hoffman, *Phys. Rev. Lett.*, in press.

[48] R. M. Diamond, *in* **Nuclei Off the Line of Stability**, R. A. Meyer and D. S. Brenner, eds., (ACS Symposium Series, Washington, DC, 1986) 341.

[49] "GAMMASPHERE - A Proposal for a National Gamma Ray Facility," M.-A. Delaplanque and R. M. Diamond, eds., *Lawrence Berkeley Laboratory Publication No. PUB-5202* (1988).

LAWRENCE BERKELEY LABORATORY
TECHNICAL INFORMATION DEPARTMENT
1 CYCLOTRON ROAD
BERKELEY, CALIFORNIA 94720